

Supporting Information

Carbohydrate-binding Module *O*-Mannosylation Alters Binding Selectivity to Cellulose and Lignin

Yaohao Li,^{1,2,‡} Xiaoyang Guan,^{2,‡} Patrick K. Chaffey,^{2,‡} Yuan Ruan,² Bo Ma,¹ Shiyong Shang,³ Michael E. Himmel,⁴ Gregg T. Beckham,^{5,*} Hai Long,^{6,*} Zhongping Tan,^{1,*}

¹Institute of Materia Medica, Chinese Academy of Medical Sciences and Peking Union Medical College, Beijing, 100050, China

²Department of Chemistry and Biochemistry and BioFrontiers Institute, University of Colorado, Boulder CO 80303, United States

³School of Pharmaceutical Sciences, Tsinghua University, Beijing, 100084, China

⁴Biosciences Center, National Renewable Energy Laboratory, Golden CO 80401, United States

⁵Renewable Resources and Enabling Sciences Center, National Renewable Energy Laboratory, Golden CO 80401, United States

⁶Computational Science Center, National Renewable Energy Laboratory, Golden CO 80401, United States

‡ Equal contribution

* Corresponding authors

Gregg T. Beckham, Renewable Resources and Enabling Sciences Center, National Renewable Energy Laboratory, Golden, CO 80401 USA, +01 (303) 384-7806, gregg.beckham@nrel.gov

Hai Long, Computational Science Center, National Renewable Energy Laboratory, Golden, CO 80401 USA, +01 (303) 384-7806, hai.long@nrel.gov

Zhongping Tan, Institute of Materia Medica, Chinese Academy of Medical Sciences and Peking Union Medical College, Beijing, 100050, China, +86 (010) 8316-6211, zhongping.tan@imm.pumc.edu.cn

I. Binding Affinity

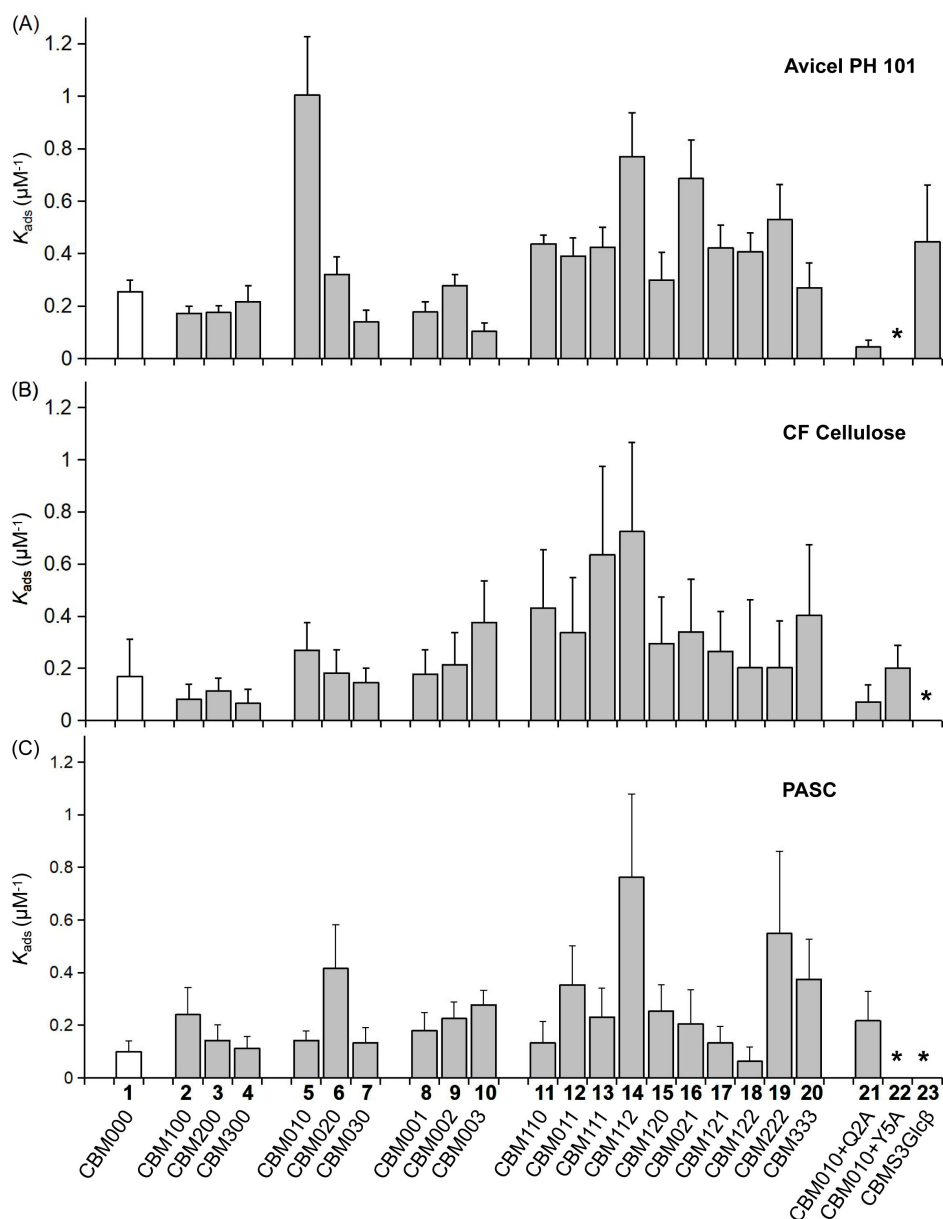


Figure S1. Direct comparison of the K_{ads} values of the glycosylated and unglycosylated CBMs on (A) commercially available Avicel PH 101 cellulose, (B) Clean-Fractionation derived cellulose (CF cellulose), and (C) phosphoric acid swollen cellulose (PASC) at 4°C. Bold numbers represent the identity of CBM glycoforms as per Fig. 2 (main text). The glycosylated CBMs were divided into 5 groups based on the differences in their glycosylation pattern. **2-4**, **5-7**, and **8-10** are O-mannosylated at one site, Thr1, Ser3, or Ser14. **11-20** are O-mannosylated at more than one site. **21-23** are modified by other O-linked glycans and mutation. More detailed structural features of each CBM isoform are indicated by its name, *i.e.*, CBM100 representing the isoform containing a single mannose at Thr1, CBM111 represents the isoform containing a single mannose at Thr1, Ser3, and Ser14, CBM010+Q2A representing the isoform containing a single mannose α -linked to Ser3 and a Gln-to-Ala mutation at position 2, and CBMS3Glc β representing the isoform containing a single glucose β -linked to Ser3. * No observable binding noted. Error bars show variance between three independent trials.

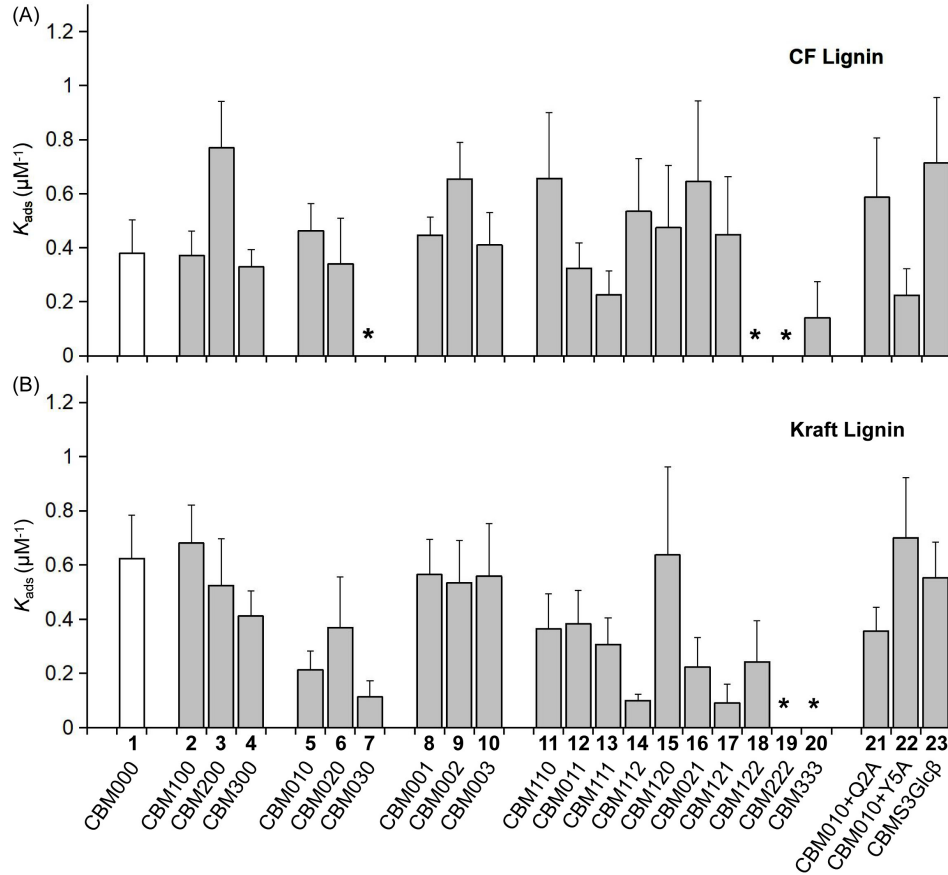


Figure S2. Direct comparison of the K_{ads} values of the glycosylated and unglycosylated CBMs on (A) Clean-Fractionation derived lignin (CF Lignin) and (B) commercially available Kraft lignin at 4°C. Bold numbers represent the identity of CBM molecules as per Fig. 2 (main text). The glycosylated CBMs were divided into 5 groups based on the differences in their glycosylation pattern. **2-4**, **5-7**, and **8-10** are O-mannosylated at one site, Thr1, Ser3, or Ser14. **11-20** are O-mannosylated at more than one site. **21-23** are modified by other O-linked glycans and mutation. More detailed structural features of each CBM isoform was implied by its name, *i.e.*, CBM100 representing the isoform containing a single mannose at Thr1, CBM111 representing the isoform containing a single mannose at Thr1, Ser3, and Ser14, CBM10+Q2A representing the isoform containing a single mannose α -linked to Ser3 and a Gln-to-Ala mutation at position 2, and CBMS3Glc β representing the isoform containing a single glucose β -linked to Ser3. * No observable binding noted. Error bars show variance between three independent trials.

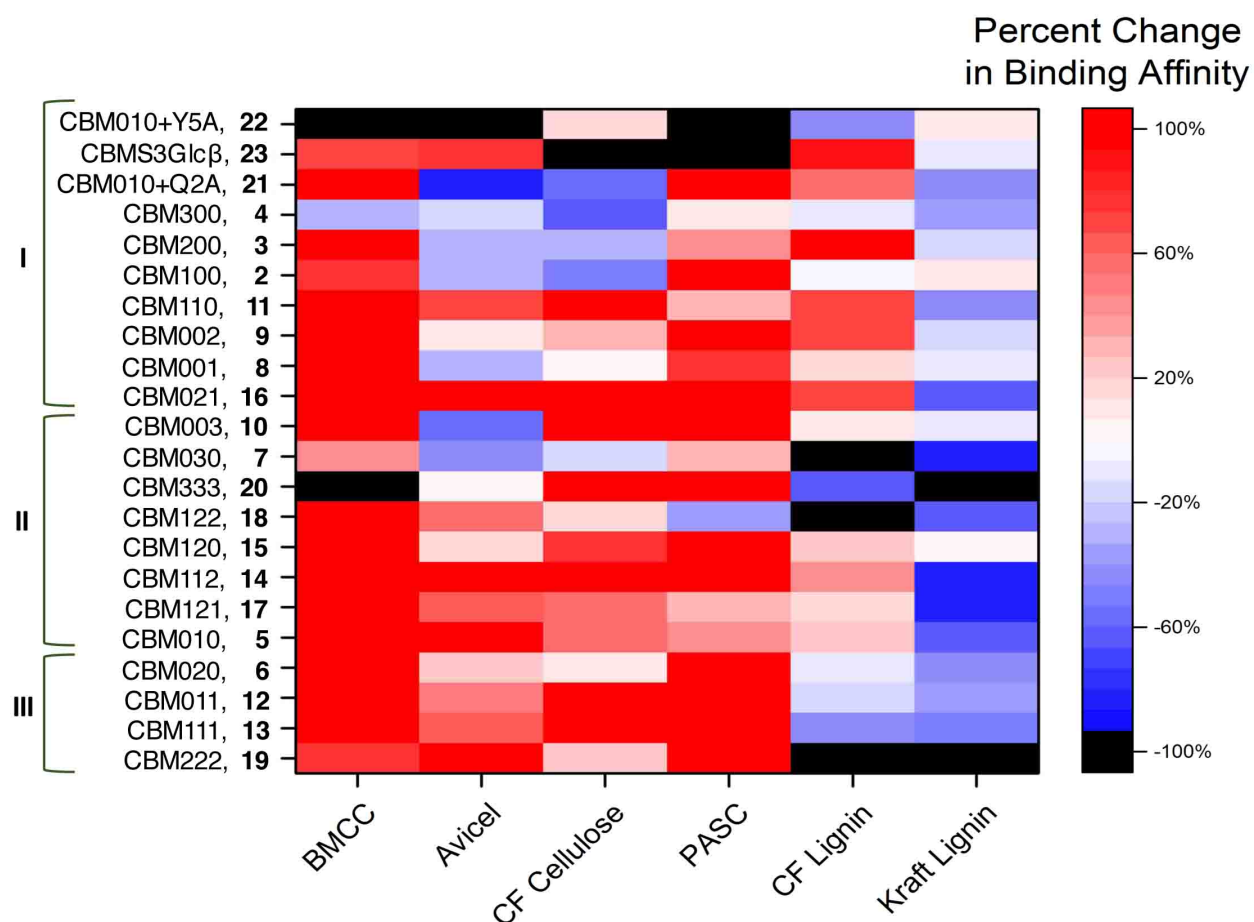


Figure S3. Changes in binding affinities caused by glycosylation at 4°C. Percent change in binding affinity towards the given substrates for each CBM glycoform relative to unglycosylated CBM 1 expressed as a heat map. Compared to Figure 3 in the main text, additional binding data for bacterial microcrystalline cellulose (BMCC) is added here ^{1, 2}. Color varies from red (indicating a 100% or more increase in binding affinity) to white (indicating no change in binding affinity) to blue (indicating an almost 100% decrease in binding affinity). Black is for CBM glycoform substrate pairs that displayed complete loss of binding. Although the order is slightly different to take into account the additional data, CBM glycoforms are ordered with the same purpose as those of Figure 4 in the main text so that poor cellulose binders are at the top, unselective binders to cellulose and lignin are in the middle, and CBMs highly selective for binding to cellulose at the bottom.

Table S1: Binding affinity values at 4°C – Numerical data represented by bars in Figure S1.

		Avicel PH 101		CF Cellulose		PASC	
		Binding Affinity (K_{ads} , μM^{-1})	B_{max} ($\mu\text{mol/g}$)	Binding Affinity (K_{ads} , μM^{-1})	B_{max} ($\mu\text{mol/g}$)	Binding Affinity (K_{ads} , μM^{-1})	B_{max} ($\mu\text{mol/g}$)
1	CBM000	0.26 ± 0.04	11.66 ± 0.93	0.17 ± 0.14	14.72 ± 6.40	0.10 ± 0.04	12.39 ± 2.82
2	CBM100	0.17 ± 0.03	23.99 ± 2.16	0.08 ± 0.06	16.73 ± 7.30	0.24 ± 0.10	9.61 ± 1.75
3	CBM200	0.17 ± 0.03	13.53 ± 1.00	0.11 ± 0.05	10.52 ± 2.28	0.14 ± 0.06	7.69 ± 1.41
4	CBM300	0.22 ± 0.06	10.71 ± 1.40	0.07 ± 0.05	9.83 ± 4.79	0.11 ± 0.05	13.58 ± 3.30
5	CBM010	1.01 ± 0.22	10.39 ± 0.92	0.27 ± 0.11	9.16 ± 1.67	0.14 ± 0.04	14.46 ± 1.94
6	CBM020	0.32 ± 0.07	10.37 ± 0.94	0.18 ± 0.09	10.25 ± 2.48	0.42 ± 0.17	7.95 ± 1.81
7	CBM030	0.14 ± 0.05	9.39 ± 1.51	0.15 ± 0.05	8.29 ± 1.52	0.13 ± 0.06	7.97 ± 1.65
8	CBM001	0.18 ± 0.04	16.57 ± 1.87	0.18 ± 0.09	5.62 ± 1.25	0.18 ± 0.07	10.69 ± 2.07
9	CBM002	0.28 ± 0.04	12.61 ± 0.96	0.21 ± 0.12	7.25 ± 1.83	0.23 ± 0.06	11.02 ± 1.43
10	CBM003	0.10 ± 0.03	16.72 ± 2.96	0.38 ± 0.16	5.26 ± 0.85	0.28 ± 0.05	12.67 ± 1.10
11	CBM110	0.44 ± 0.03	16.00 ± 0.65	0.43 ± 0.22	9.68 ± 2.26	0.13 ± 0.08	21.90 ± 7.64
12	CBM011	0.39 ± 0.07	16.88 ± 1.28	0.34 ± 0.21	7.06 ± 1.75	0.35 ± 0.15	13.29 ± 2.53
13	CBM111	0.42 ± 0.08	16.35 ± 1.32	0.64 ± 0.34	8.42 ± 2.51	0.23 ± 0.11	11.52 ± 2.49
14	CBM112	0.77 ± 0.17	15.72 ± 1.93	0.72 ± 0.34	8.14 ± 1.80	0.76 ± 0.32	15.63 ± 4.84
15	CBM120	0.30 ± 0.11	8.42 ± 1.36	0.29 ± 0.18	9.66 ± 3.11	0.25 ± 0.10	15.76 ± 2.89
16	CBM021	0.69 ± 0.15	8.89 ± 0.89	0.34 ± 0.20	10.93 ± 3.39	0.21 ± 0.13	12.41 ± 3.66
17	CBM121	0.42 ± 0.09	13.49 ± 1.16	0.26 ± 0.15	14.58 ± 4.01	0.13 ± 0.06	25.20 ± 6.87
18	CBM122	0.41 ± 0.07	12.61 ± 0.95	0.20 ± 0.26	4.95 ± 3.13	0.06 ± 0.06	13.80 ± 7.70
19	CBM222	0.53 ± 0.13	9.33 ± 0.99	0.20 ± 0.18	8.19 ± 2.92	0.55 ± 0.31	10.88 ± 2.76
20	CBM333	0.27 ± 0.09	6.03 ± 1.02	0.40 ± 0.27	8.19 ± 2.47	0.37 ± 0.15	6.83 ± 1.59
21	CBM010+Q2A	0.04 ± 0.03	29.01 ± 12.50	0.07 ± 0.06	9.13 ± 3.81	0.22 ± 0.11	8.75 ± 2.07
22	CBM010+Y5A	*	*	0.20 ± 0.09	7.10 ± 1.49	*	*
23	CBMS3Glcβ	0.45 ± 0.22	4.95 ± 0.89	*	*	*	*

* No observable binding noted.

Table S2: Binding affinity values at 4°C – Numerical data represented by bars in Figure S2.

		CF Lignin		Kraft Lignin	
		Binding Affinity (K_{ads} , μM^{-1})	B_{max} ($\mu\text{mol/g}$)	Binding Affinity (K_{ads} , μM^{-1})	B_{max} ($\mu\text{mol/g}$)
1	CBM000	0.38 ± 0.12	10.63 ± 1.61	0.62 ± 0.16	11.37 ± 1.90
2	CBM100	0.37 ± 0.09	10.73 ± 1.03	0.68 ± 0.14	8.95 ± 0.83
3	CBM200	0.77 ± 0.17	8.50 ± 0.95	0.53 ± 0.17	9.33 ± 1.21
4	CBM300	0.33 ± 0.06	12.21 ± 1.01	0.41 ± 0.09	9.43 ± 0.83
5	CBM010	0.46 ± 0.10	8.48 ± 0.81	0.21 ± 0.07	9.69 ± 1.37
6	CBM020	0.34 ± 0.17	4.79 ± 1.23	0.37 ± 0.19	6.98 ± 1.98
7	CBM030	*	*	0.11 ± 0.06	10.17 ± 2.79
8	CBM001	0.45 ± 0.07	9.92 ± 0.66	0.57 ± 0.13	9.84 ± 1.08
9	CBM002	0.65 ± 0.14	5.75 ± 0.58	0.53 ± 0.16	11.54 ± 1.79
10	CBM003	0.41 ± 0.12	7.81 ± 0.92	0.56 ± 0.19	5.57 ± 0.74
11	CBM110	0.66 ± 0.24	6.40 ± 1.84	0.36 ± 0.13	7.98 ± 1.25
12	CBM011	0.32 ± 0.09	8.86 ± 1.20	0.38 ± 0.12	6.09 ± 0.92
13	CBM111	0.23 ± 0.09	7.07 ± 1.17	0.31 ± 0.10	5.94 ± 0.85
14	CBM112	0.53 ± 0.19	5.25 ± 1.00	0.10 ± 0.02	19.46 ± 2.50
15	CBM120	0.47 ± 0.23	7.77 ± 3.81	0.64 ± 0.32	4.62 ± 3.95
16	CBM021	0.64 ± 0.30	3.19 ± 0.66	0.22 ± 0.11	4.93 ± 1.13
17	CBM121	0.45 ± 0.21	6.11 ± 1.97	0.09 ± 0.07	7.78 ± 3.32
18	CBM122	*	*	0.24 ± 0.15	3.72 ± 1.23
19	CBM222	*	*	*	*
20	CBM333	0.14 ± 0.13	5.25 ± 2.84	*	*
21	CBM010+Q2A	0.59 ± 0.22	6.10 ± 1.09	0.36 ± 0.09	7.83 ± 0.78
22	CBM010+Y5A	0.22 ± 0.10	5.93 ± 1.16	0.70 ± 0.22	6.48 ± 1.52
23	CBMS3Glcβ	0.71 ± 0.24	5.24 ± 0.71	0.55 ± 0.13	5.63 ± 0.62

* No observable binding noted.

Table S3: Percent Change in Binding Affinities at 4°C – Numerical data represented in Figure 4 and Figure S3.

		BMCC[#]	Avicel PH 101	CF Cellulose	PASC	CF Lignin	Kraft Lignin
2	CBM100	79%	-32%	-52%	140%	-2%	9%
3	CBM200	280%	-31%	-32%	42%	102%	-16%
4	CBM300	-33%	-15%	-61%	12%	-13%	-34%
5	CBM010	347%	294%	59%	42%	22%	-66%
6	CBM020	135%	26%	8%	316%	-10%	-41%
7	CBM030	45%	-45%	-14%	33%	-100%	-82%
8	CBM001	291%	-30%	5%	79%	17%	-9%
9	CBM002	247%	9%	27%	125%	72%	-14%
10	CBM003	180%	-60%	122%	177%	8%	-10%
11	CBM110	113%	72%	156%	33%	73%	-42%
12	CBM011	200%	53%	100%	254%	-15%	-39%
13	CBM111	638%	66%	276%	131%	-41%	-51%
14	CBM112	317%	202%	329%	663%	41%	-84%
15	CBM120	174%	17%	74%	153%	25%	2%
16	CBM021	113%	169%	102%	106%	70%	-64%
17	CBM121	549%	65%	57%	32%	18%	-85%
18	CBM122	146%	60%	20%	-38%	-100%	-61%
19	CBM222	73%	108%	21%	449%	-100%	-100%
20	CBM333	-100%	6%	139%	275%	-63%	-100%
21	CBM010+Q2A	269%	-83%	-58%	117%	54%	-43%
22	CBM010+Y5A	-100%	-100%	19%	-100%	-41%	12%
23	CBMS3Glc β	68%	75%	-100%	-100%	88%	-11%

[#] Data calculated based on previous studies.^{1, 2}

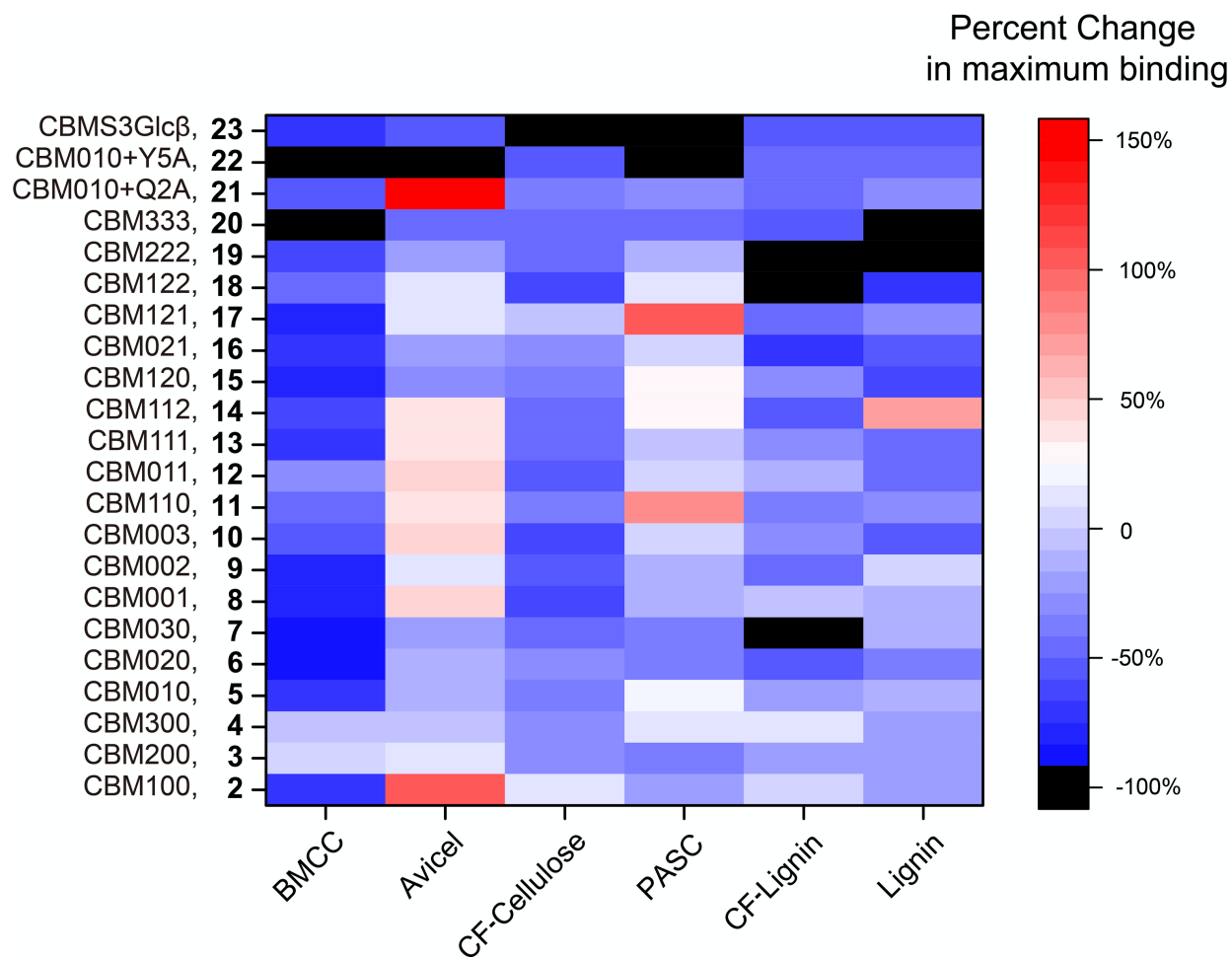


Figure S4. Changes in maximum binding (B_{max}) caused by glycosylation at 4°C. Percent change in B_{max} towards the given substrates for each CBM glycoform relative to unglycosylated CBM 1 expressed as a heat map. Color varies from red (indicating a 100% or more increase in B_{max}) to white (indicating no change in B_{max}) to blue (indicating an almost 100% decrease in B_{max}). CBM glycoforms are ordered according to the numbering in the main text. B_{max} data for bacterial microcrystalline cellulose (BMCC) is calculated based on previous studies.^{1,2}

Table S4: Percent Change in maximum binding (*B*_{max}) at 4°C – Numerical data represented in Figure S4.

		BMCC[#]	Avicel PH 101	CF Cellulose	PASC	CF Lignin	Kraft Lignin
2	CBM100	-73%	106%	14%	-22%	1%	-21%
3	CBM200	4%	16%	-29%	-38%	-20%	-18%
4	CBM300	-8%	-8%	-33%	10%	15%	-17%
5	CBM010	-75%	-11%	-38%	17%	-20%	-15%
6	CBM020	-85%	-11%	-30%	-36%	-55%	-39%
7	CBM030	-88%	-19%	-44%	-36%	-100%	-11%
8	CBM001	-79%	42%	-62%	-14%	-7%	-13%
9	CBM002	-75%	8%	-51%	-11%	-46%	1%
10	CBM003	-56%	43%	-64%	2%	-27%	-51%
11	CBM110	-46%	37%	-34%	77%	-40%	-30%
12	CBM011	-33%	45%	-52%	7%	-17%	-46%
13	CBM111	-73%	40%	-43%	-7%	-33%	-48%
14	CBM112	-60%	35%	-45%	26%	-51%	71%
15	CBM120	-77%	-28%	-34%	27%	-27%	-59%
16	CBM021	-70%	-24%	-26%	0%	-70%	-57%
17	CBM121	-80%	16%	-1%	103%	-43%	-32%
18	CBM122	-44%	8%	-66%	11%	-100%	-67%
19	CBM222	-66%	-20%	-44%	-12%	-100%	-100%
20	CBM333	-100%	-48%	-44%	-45%	-51%	-100%
21	CBM010+Q2A	-54%	149%	-38%	-29%	-43%	-31%
22	CBM010+Y5A	-100%	-100%	-52%	-100%	-44%	-43%
23	CBMS3Glcβ	-69%	-58%	-100%	-100%	-51%	-50%

[#] Data calculated based on previous studies.^{1,2}

Table S5: Binding affinity values of three representative CBM glyco-variants at 30°C – The binding affinity was measured as described in the “Methods”, except that the samples were stirred to equilibrium at 30°C for 2 h.

		Avicel		Kraft Lignin	
		Binding Affinity (K_{ads} , μM^{-1})	B_{max} ($\mu\text{mol/g}$)	Binding Affinity (K_{ads} , μM^{-1})	B_{max} ($\mu\text{mol/g}$)
1	CBM000	0.29 ± 0.09	6.79 ± 0.39	0.27 ± 0.05	22.83 ± 1.28
10	CBM003	0.41 ± 0.18	5.81 ± 1.04	1.06 ± 0.85	4.10 ± 6.99
12	CBM011	0.44 ± 0.10	13.57 ± 1.82	0.25 ± 0.08	10.27 ± 1.57
14	CBM112	0.78 ± 0.30	14.03 ± 8.02	*	*

* No observable binding noted.

II. Average correlation and the Spearman's ranked correlation coefficient:

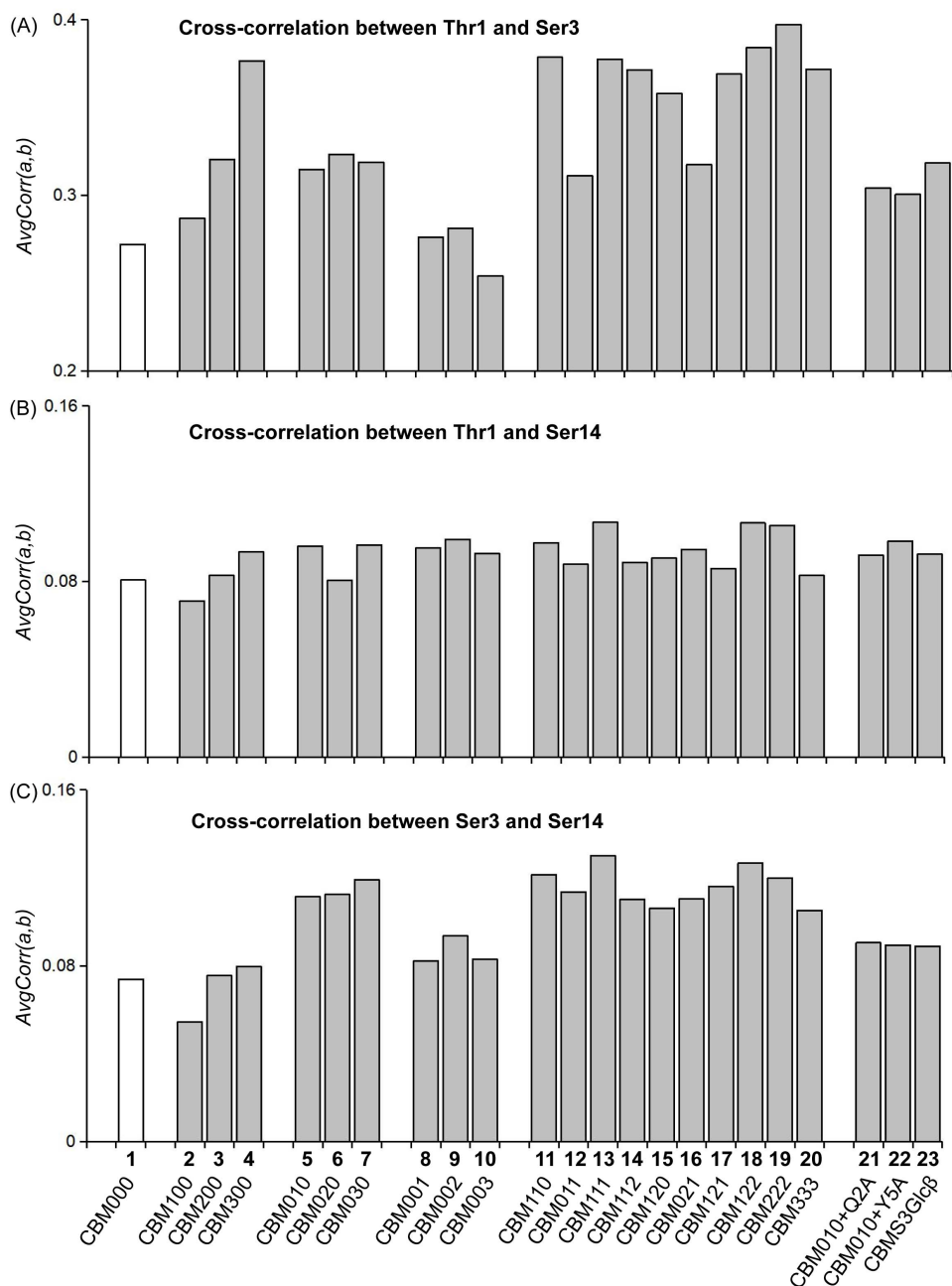


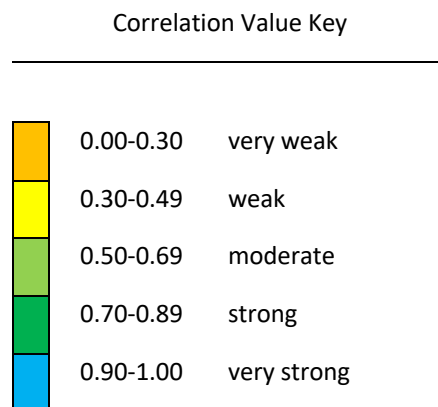
Figure S5. Cross-correlations are a function of distance at 4°C. The average correlation (*AvgCorr*) is displayed for each of the three pairs of glycosylation sites: (A) Thr1 and Ser3, (B) Thr1 and Ser14, (C) Ser3 and Ser14. Note the difference in y-axis scale between panels. These values represent how coordinated the motions of two glycosylation sites are and can vary from +1.0 to -1.0. White bar is unglycosylated, wild-type CBM.

Table S6: Calculated average correlation of motion at 4°C – Numerical data represented by bars in Figure S5.

		Correlation between:		
		Thr1 & Ser3	Thr1 & Ser14	Ser3 & Ser14
1	CBM000	0.2720	0.0806	0.0739
2	CBM100	0.2869	0.0710	0.0544
3	CBM200	0.3204	0.0827	0.0755
4	CBM300	0.3766	0.0934	0.0796
5	CBM010	0.3147	0.0960	0.1114
6	CBM020	0.3232	0.0805	0.1124
7	CBM030	0.3189	0.0966	0.1192
8	CBM001	0.2762	0.0952	0.0822
9	CBM002	0.2812	0.0991	0.0936
10	CBM003	0.2540	0.0927	0.0830
11	CBM110	0.3786	0.0975	0.1214
12	CBM011	0.3111	0.0878	0.1135
13	CBM111	0.3775	0.1069	0.1301
14	CBM112	0.3714	0.0887	0.1102
15	CBM120	0.3580	0.0906	0.1062
16	CBM021	0.3174	0.0945	0.1104
17	CBM121	0.3690	0.0858	0.1160
18	CBM122	0.3840	0.1066	0.1267
19	CBM222	0.3971	0.1054	0.1199
20	CBM333	0.3718	0.0827	0.1052
21	CBM010+Q2A	0.3041	0.0920	0.0905
22	CBM010+Y5A	0.3005	0.0983	0.0894
23	CBMS3GlcB	0.3183	0.0924	0.0889

Table S7: Calculated correlation coefficients – Numerical data represented by bars in Figure 5. Colors indicate strength of the correlations or anti-correlations: orange is very weak, yellow is weak, light green is moderate and dark green is strong.³

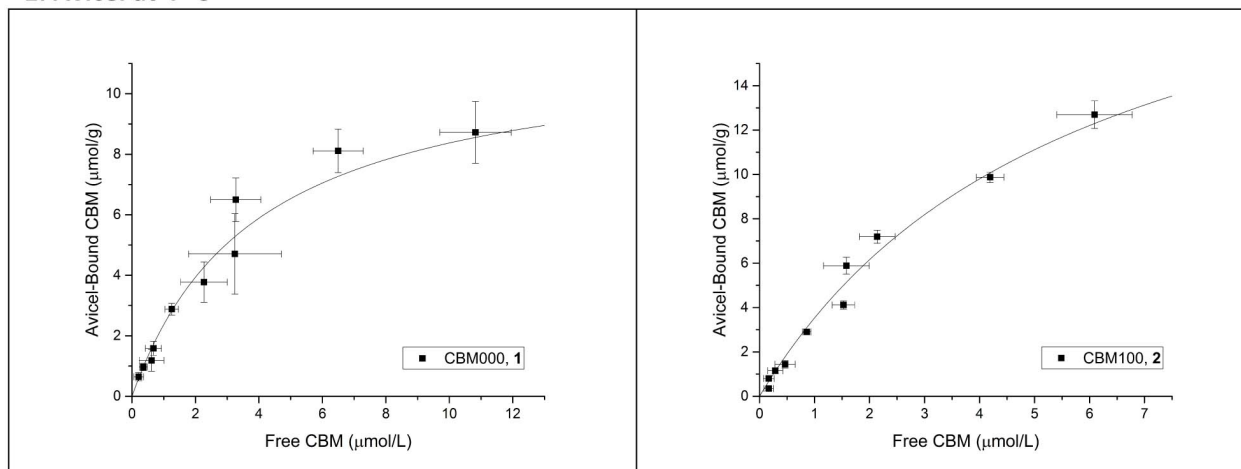
Substrate	Correlation between...		
	Thr1 & Ser3	Thr1 & Ser14	Ser3 & Ser14
Avicel	0.5089	0.2016	0.5642
CF Cell	0.2717	0.2090	0.5366
PASC	0.0875	-0.2501	0.1458
CF Lignin	-0.2502	0.2122	-0.3185
Kraft Lignin	-0.6242	-0.1812	-0.6706

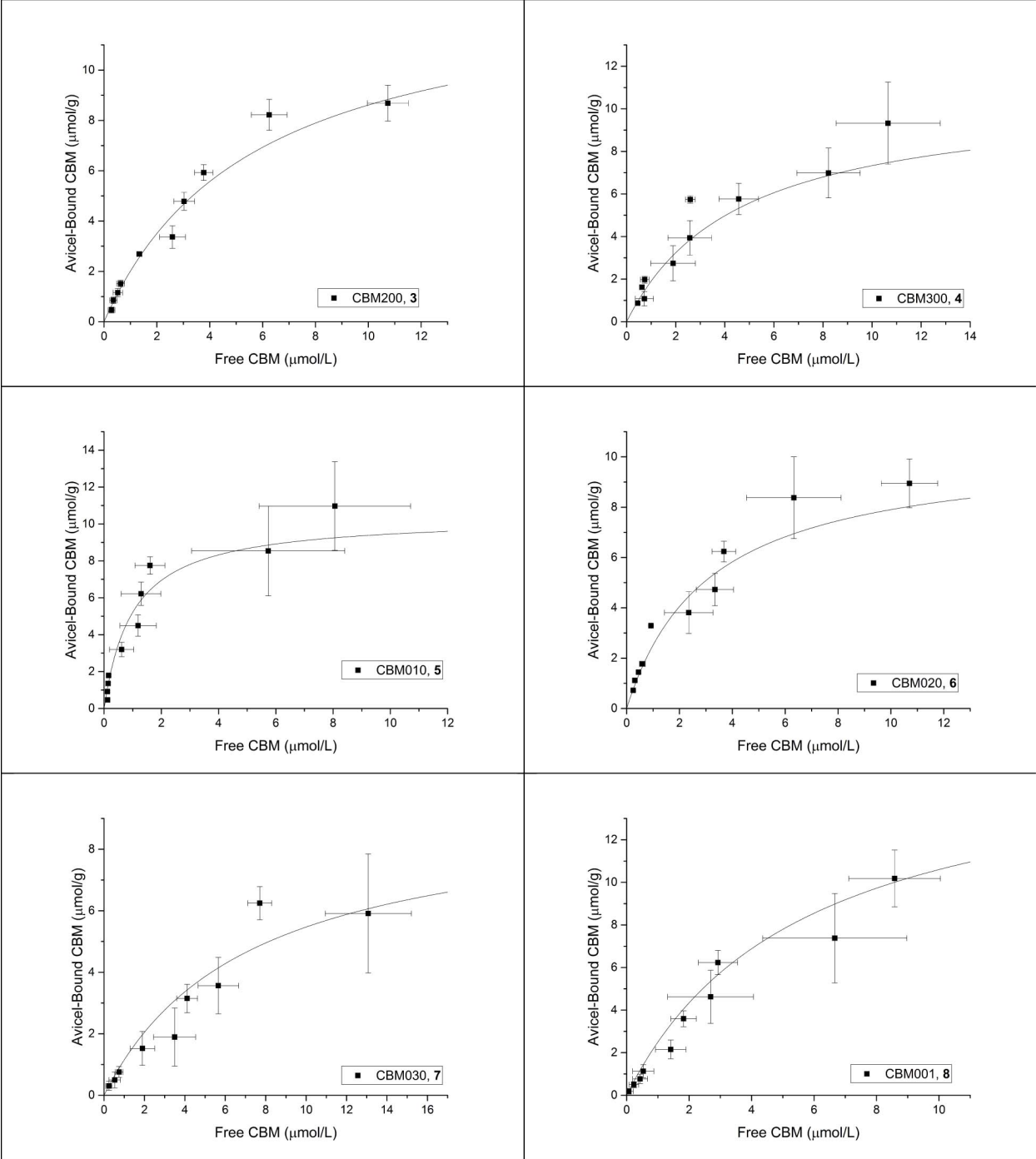


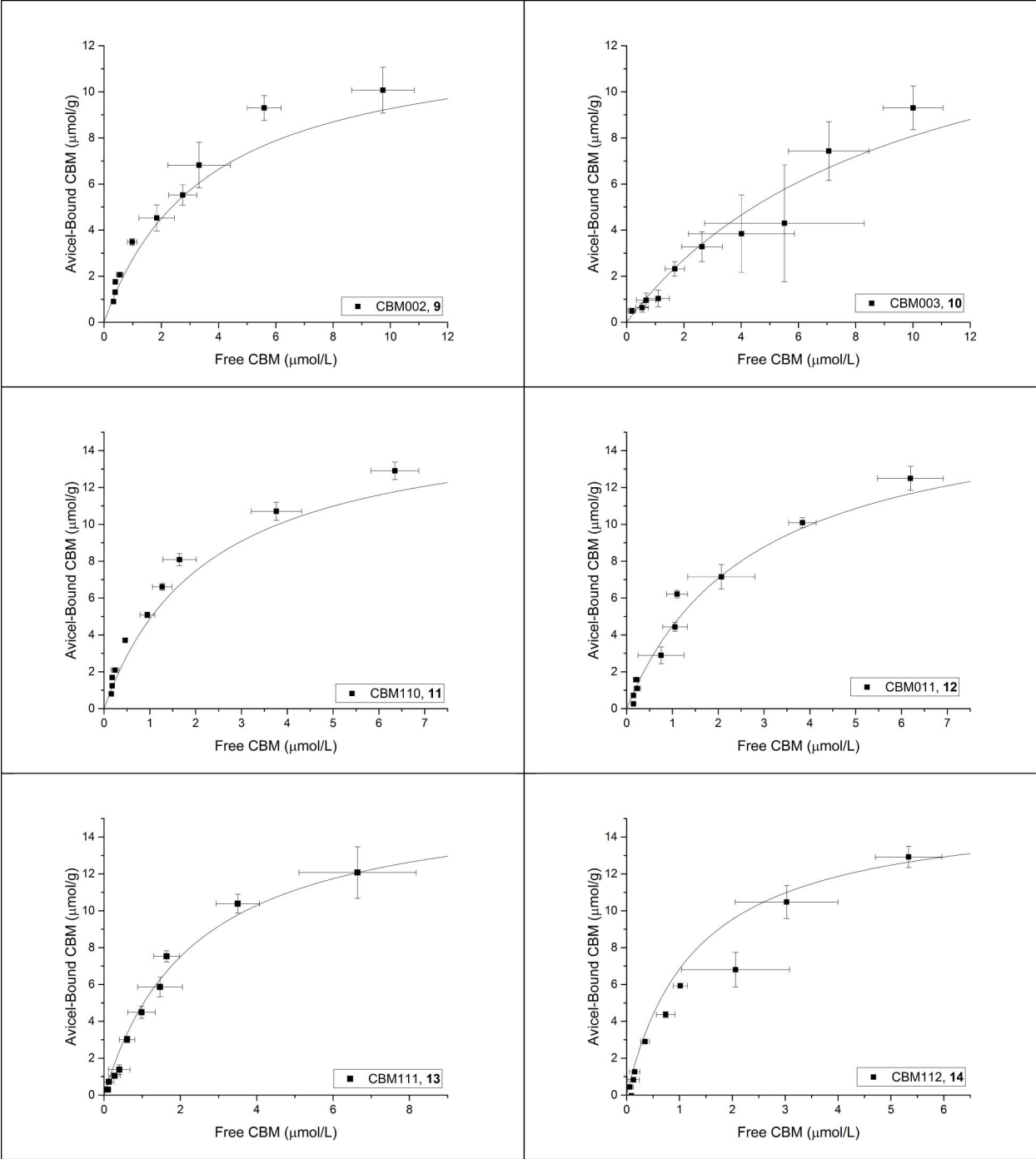
III. Adsorption isotherm plots of CBMs with different substrates

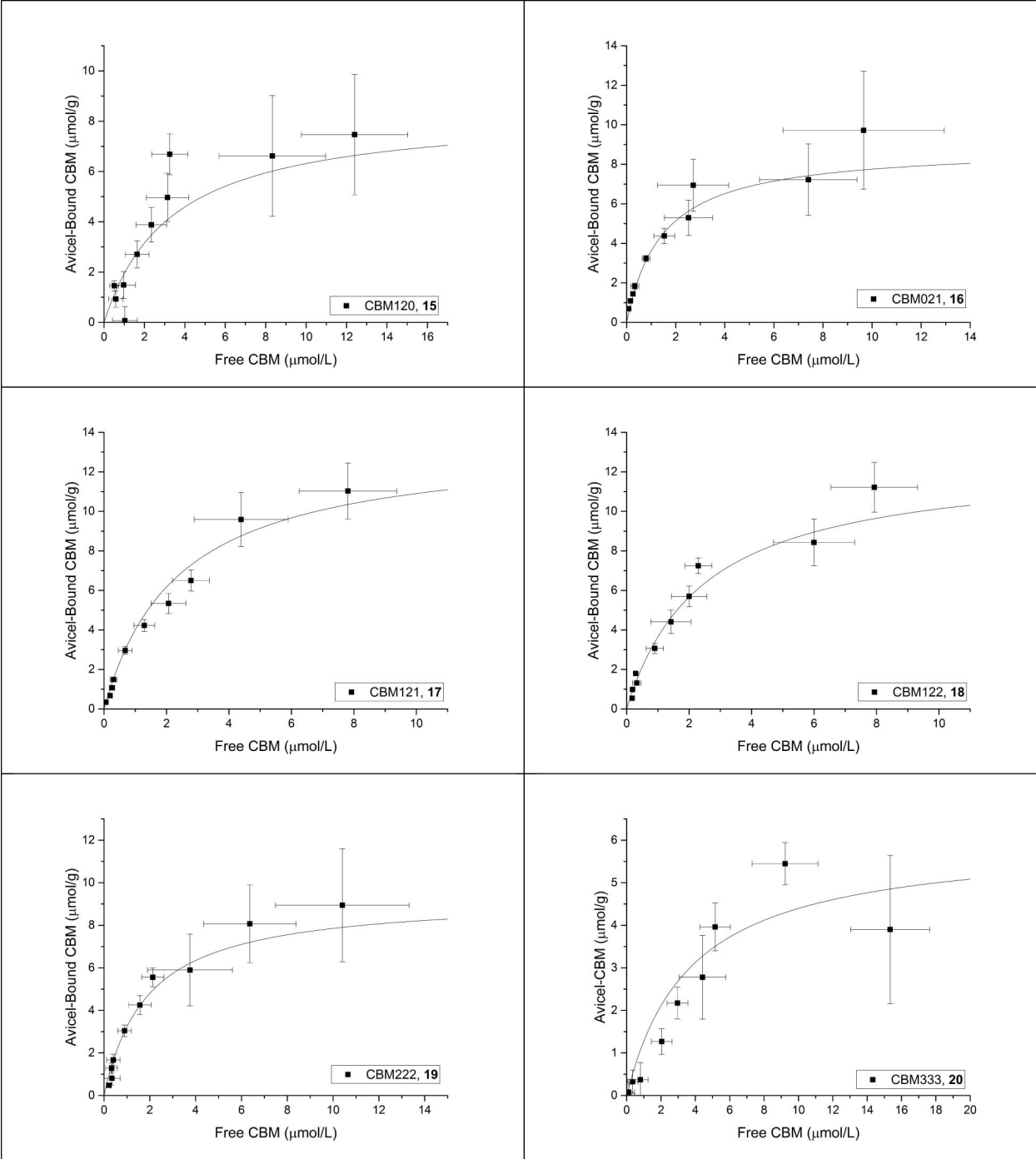
The following are the adsorption Isotherm plots of CBM variants that were obtained as previously reported.^{1,2} Data points represent averaged data of at least three trials. X-Error Bars represent the standard deviations of 'Free' concentrations. Y-Error Bars represent the standard deviations of the calculated 'Bound' concentrations.

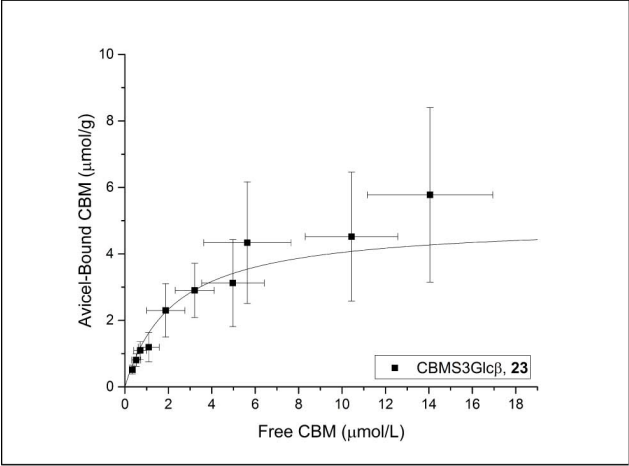
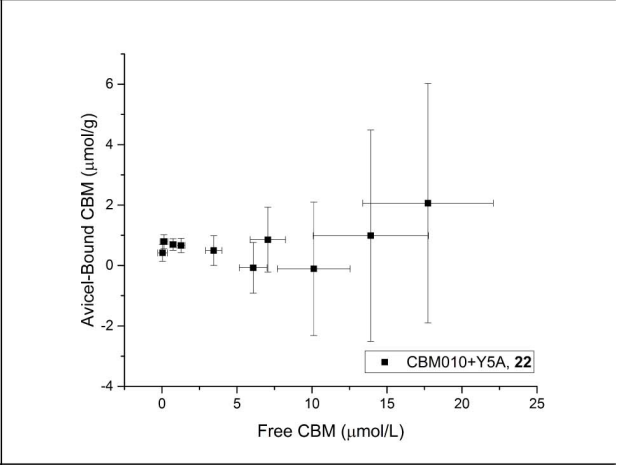
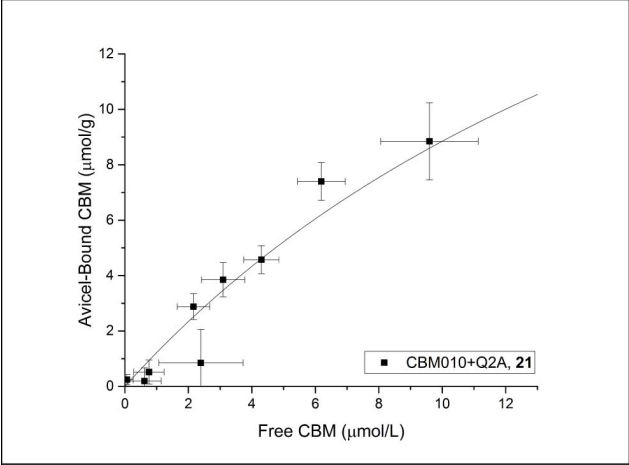
1. Avicel at 4 °C



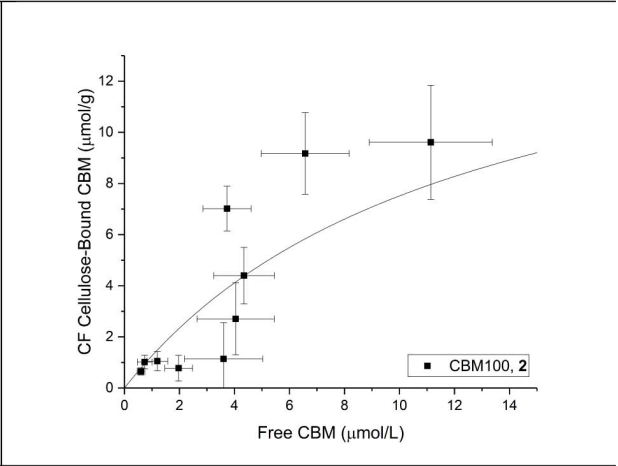
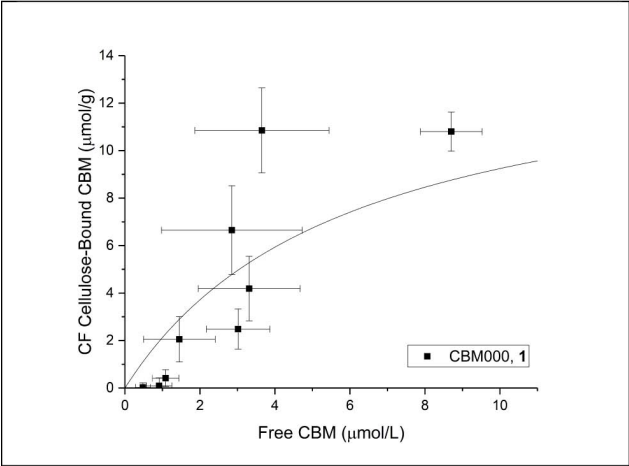


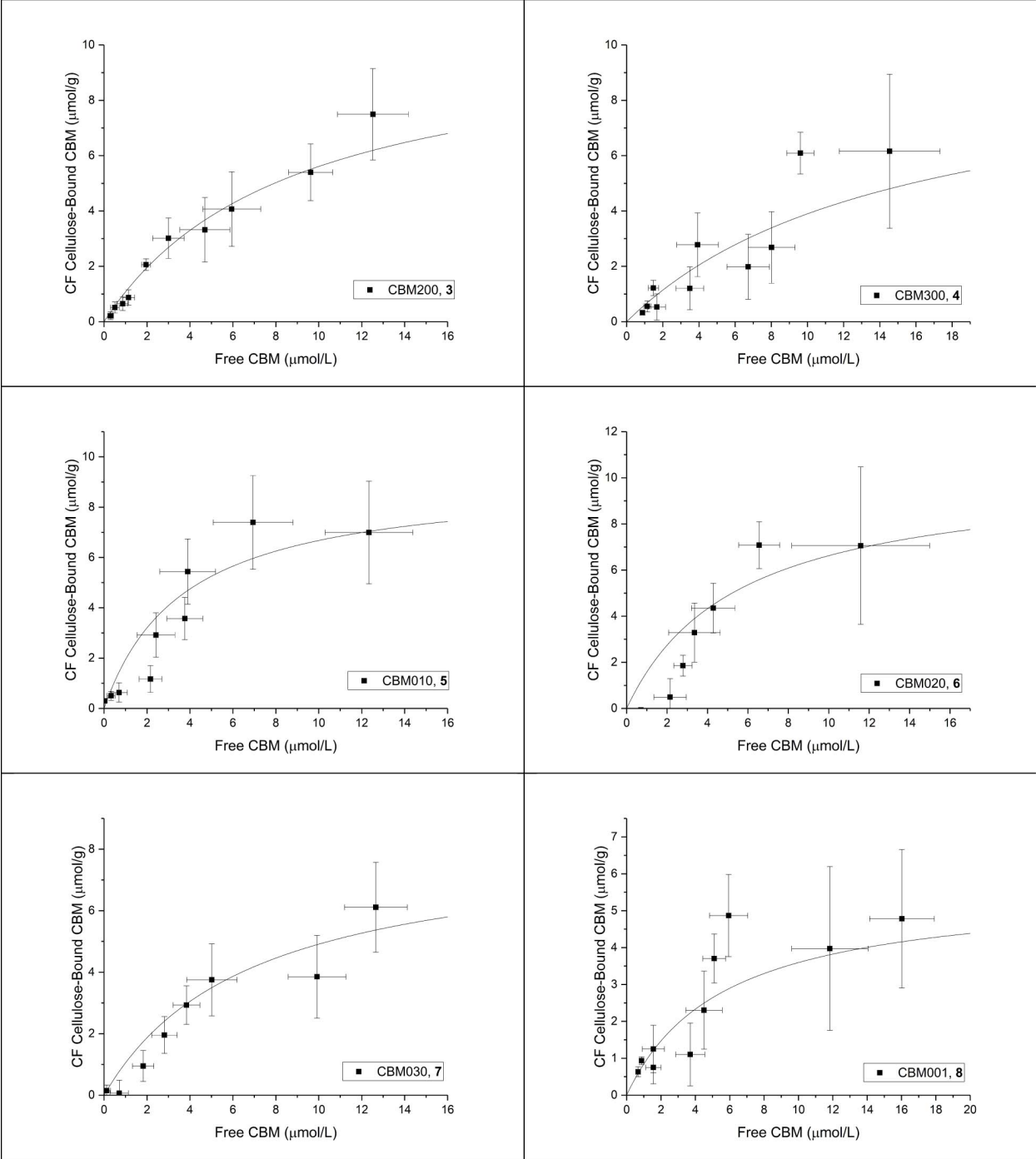


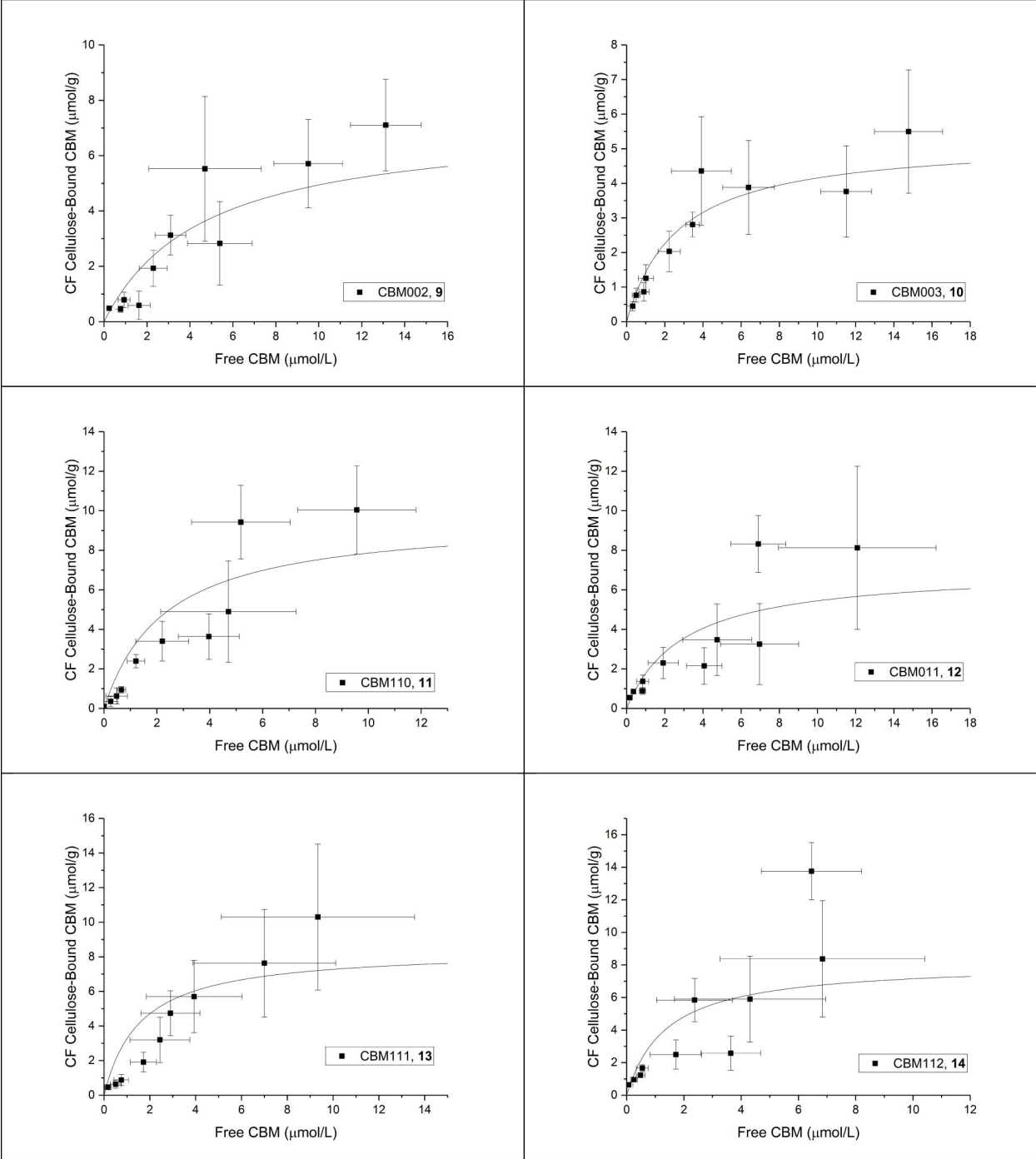


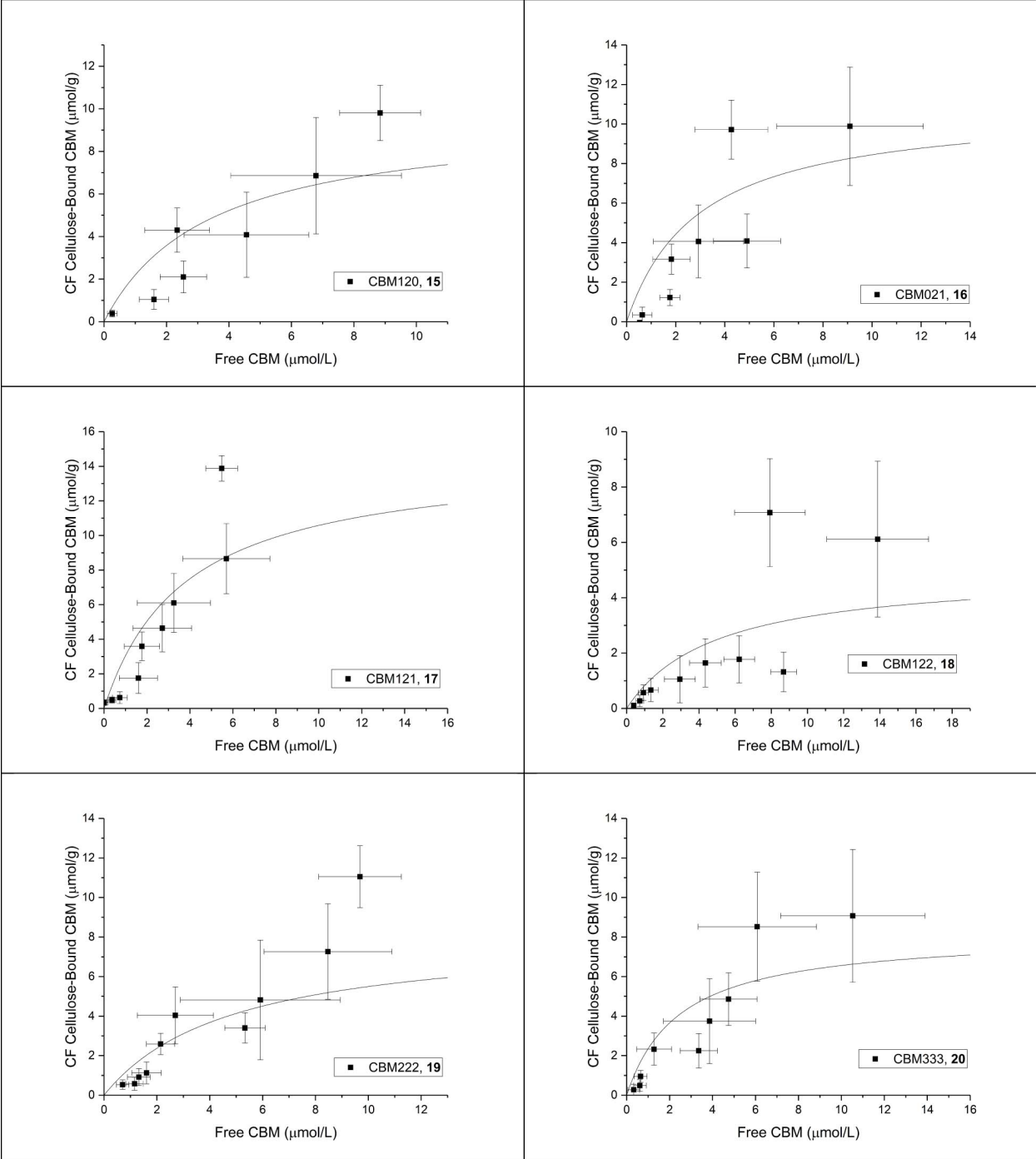


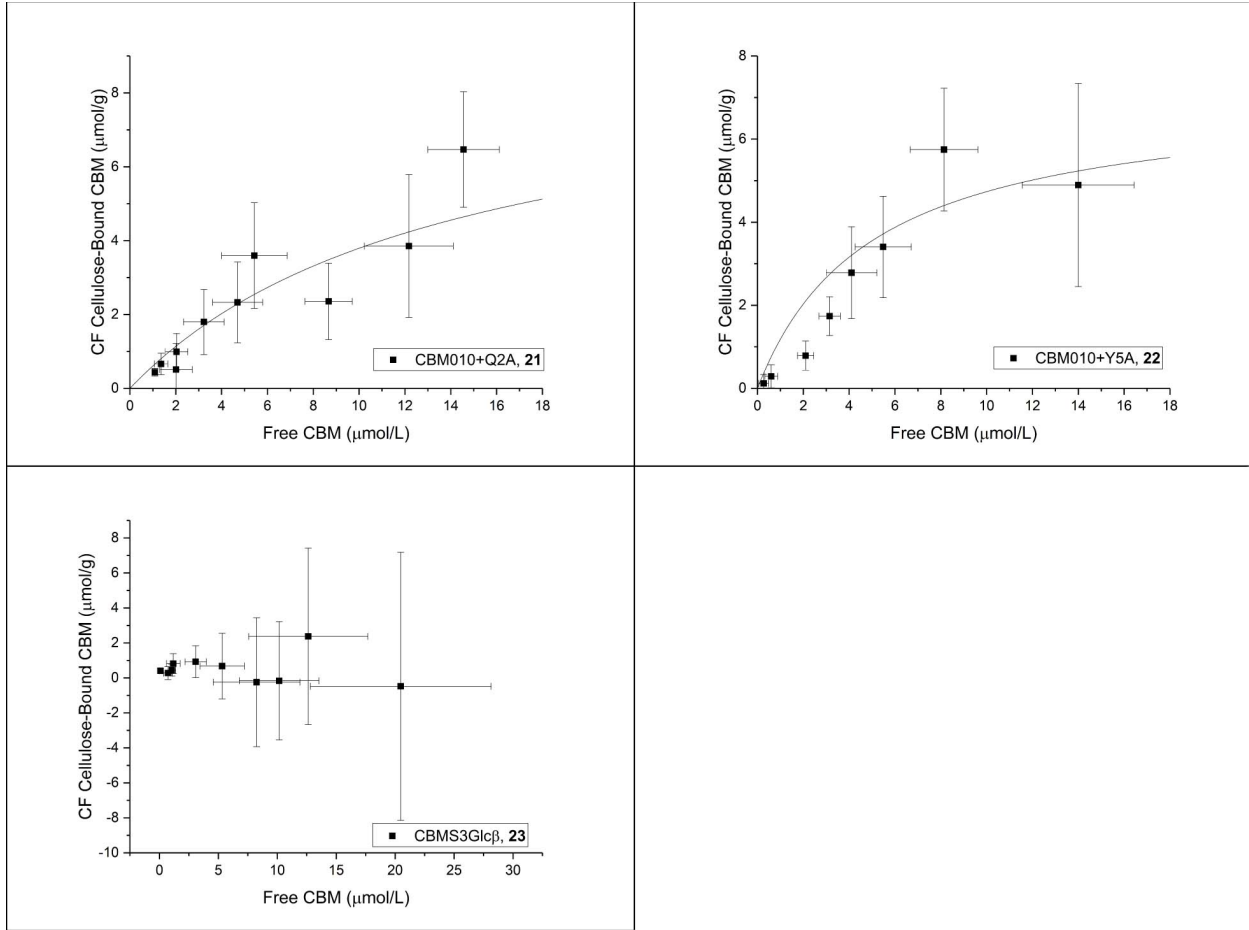
2. CF Cellulose at 4 °C



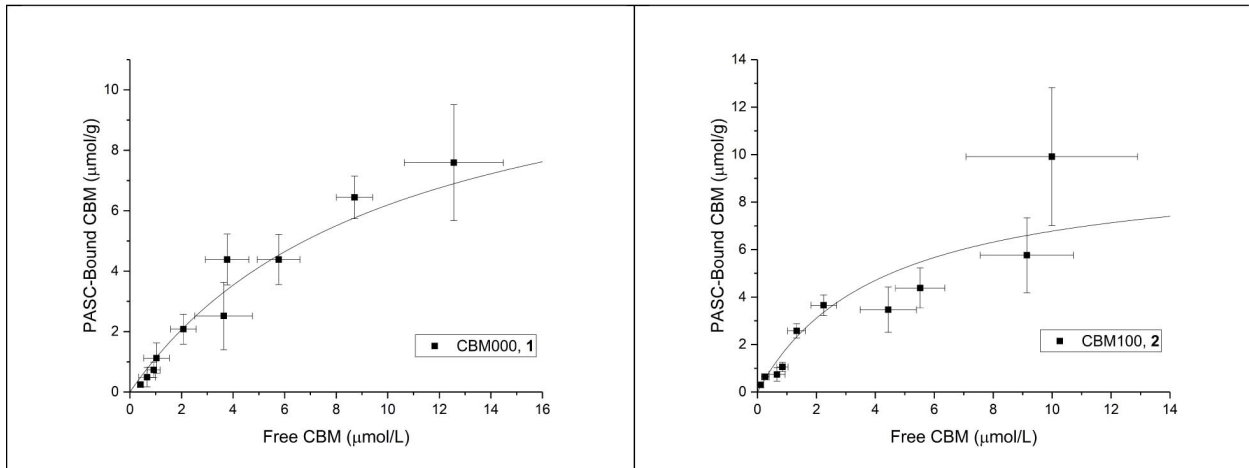


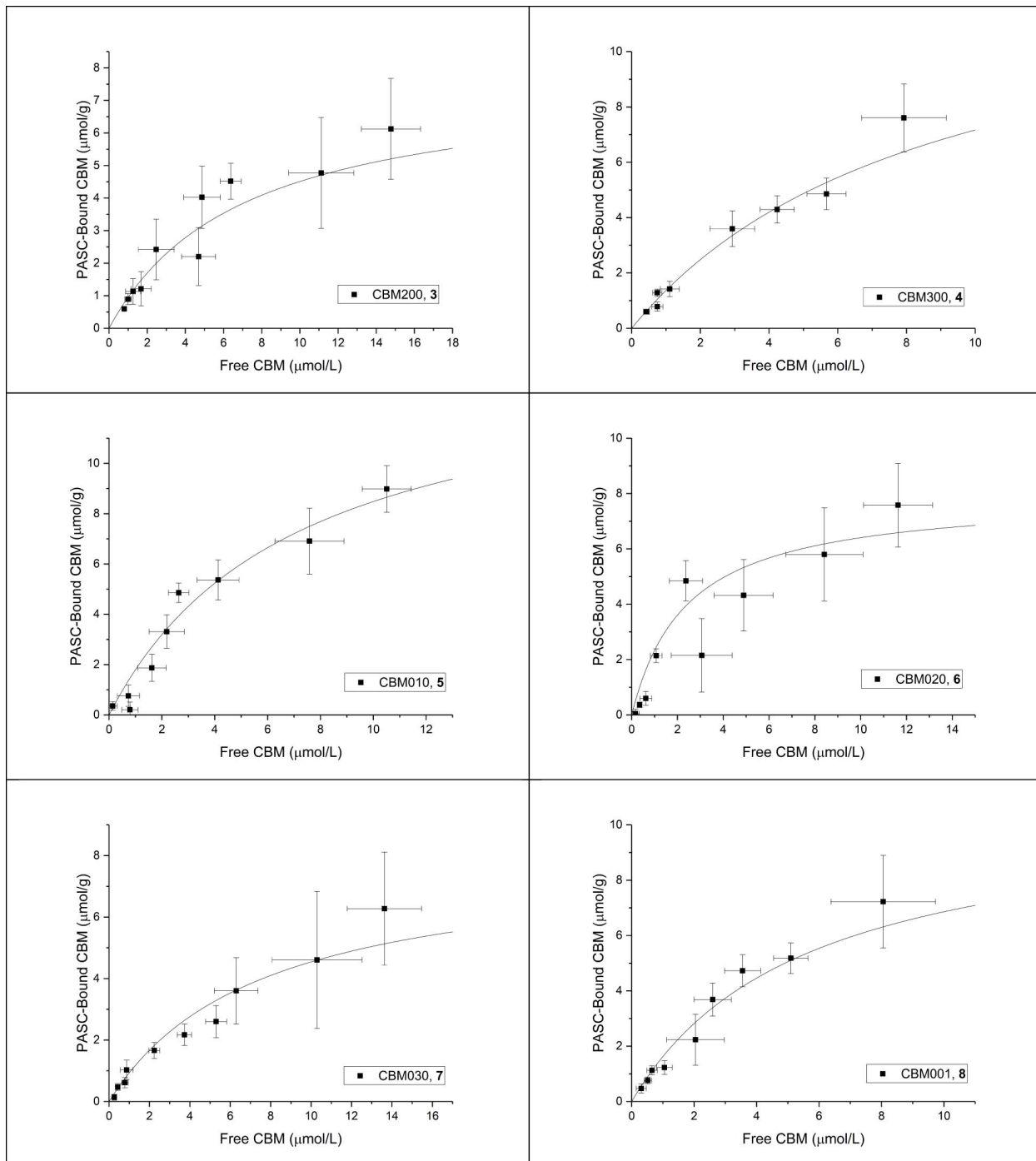


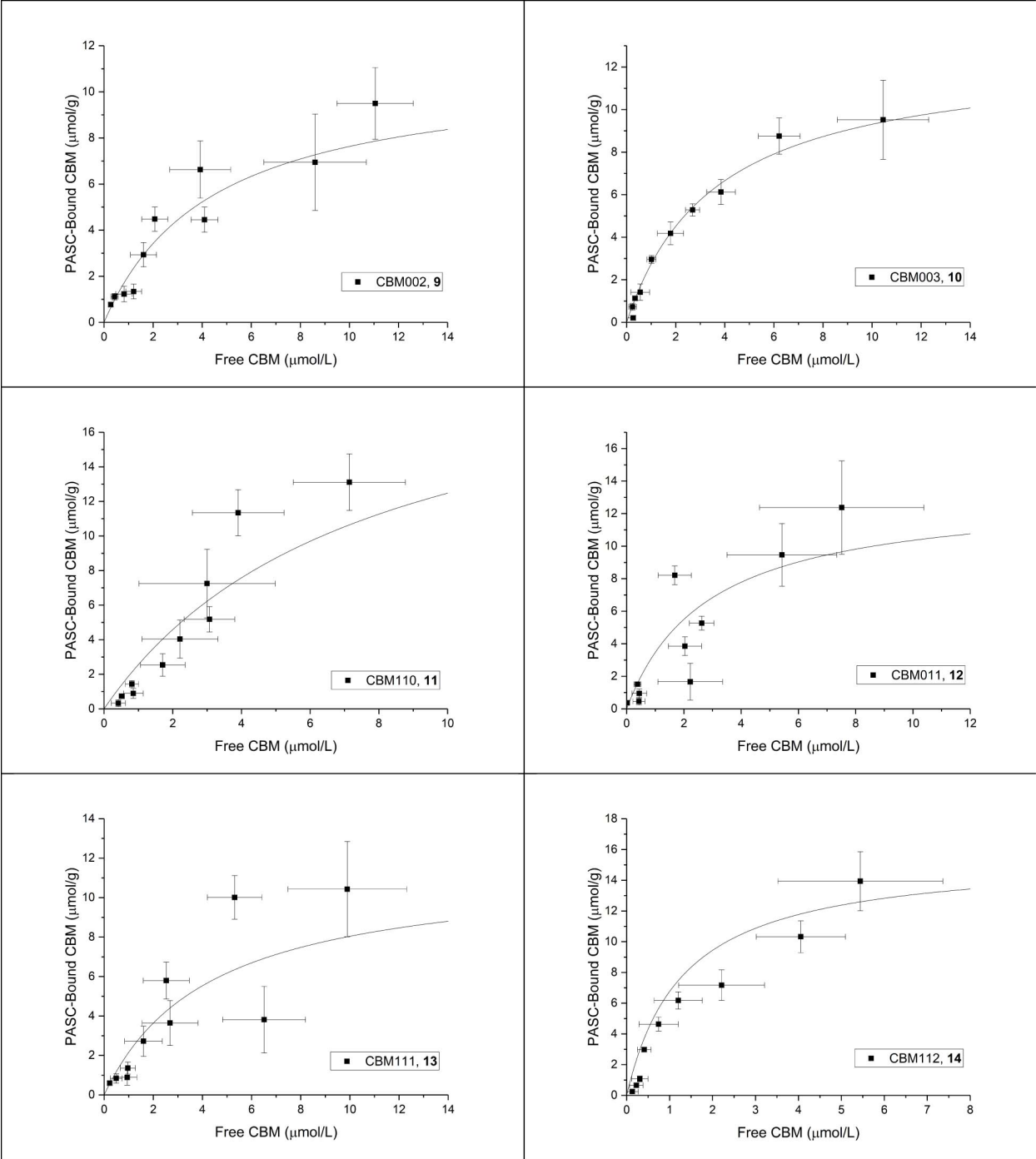


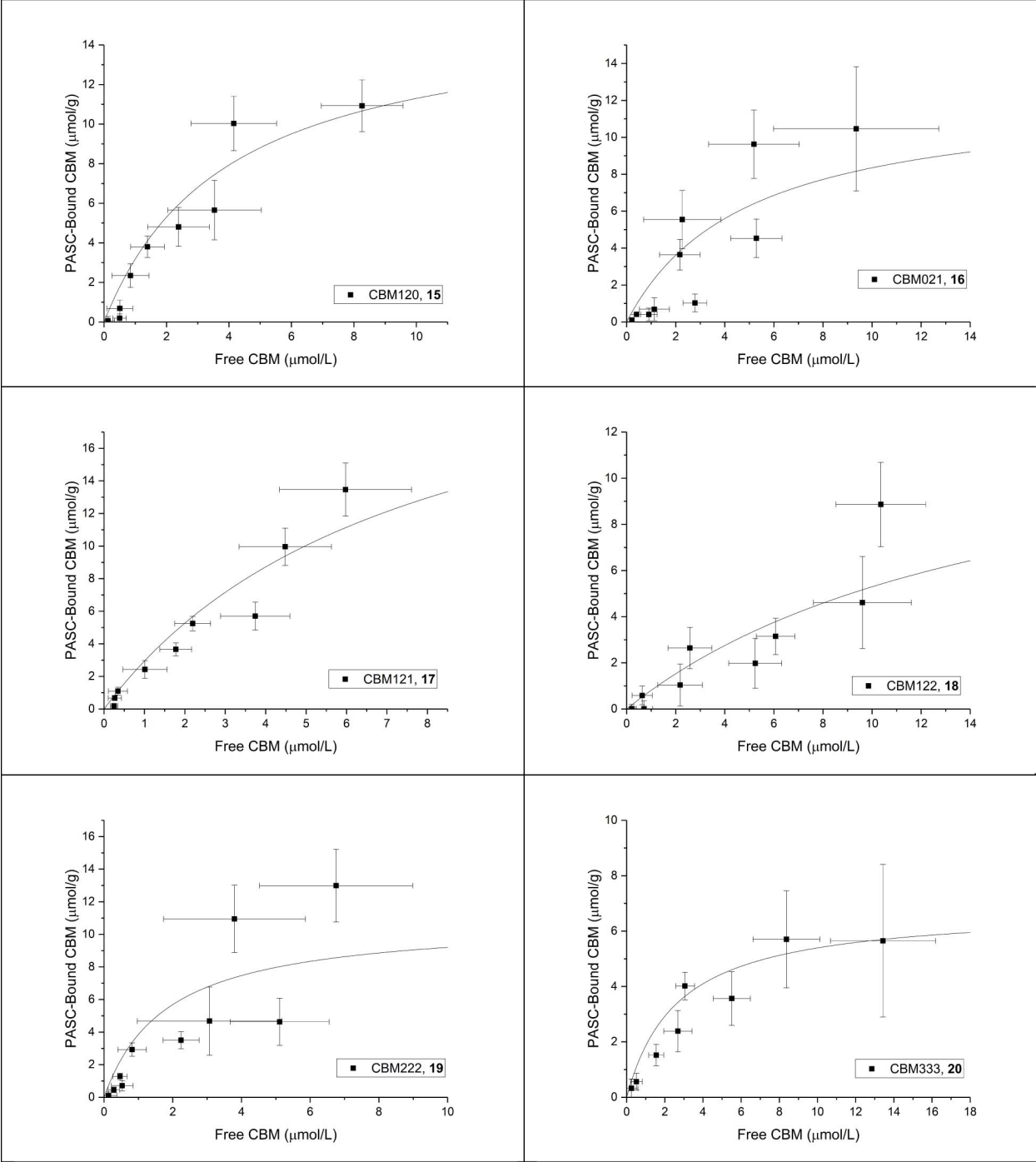


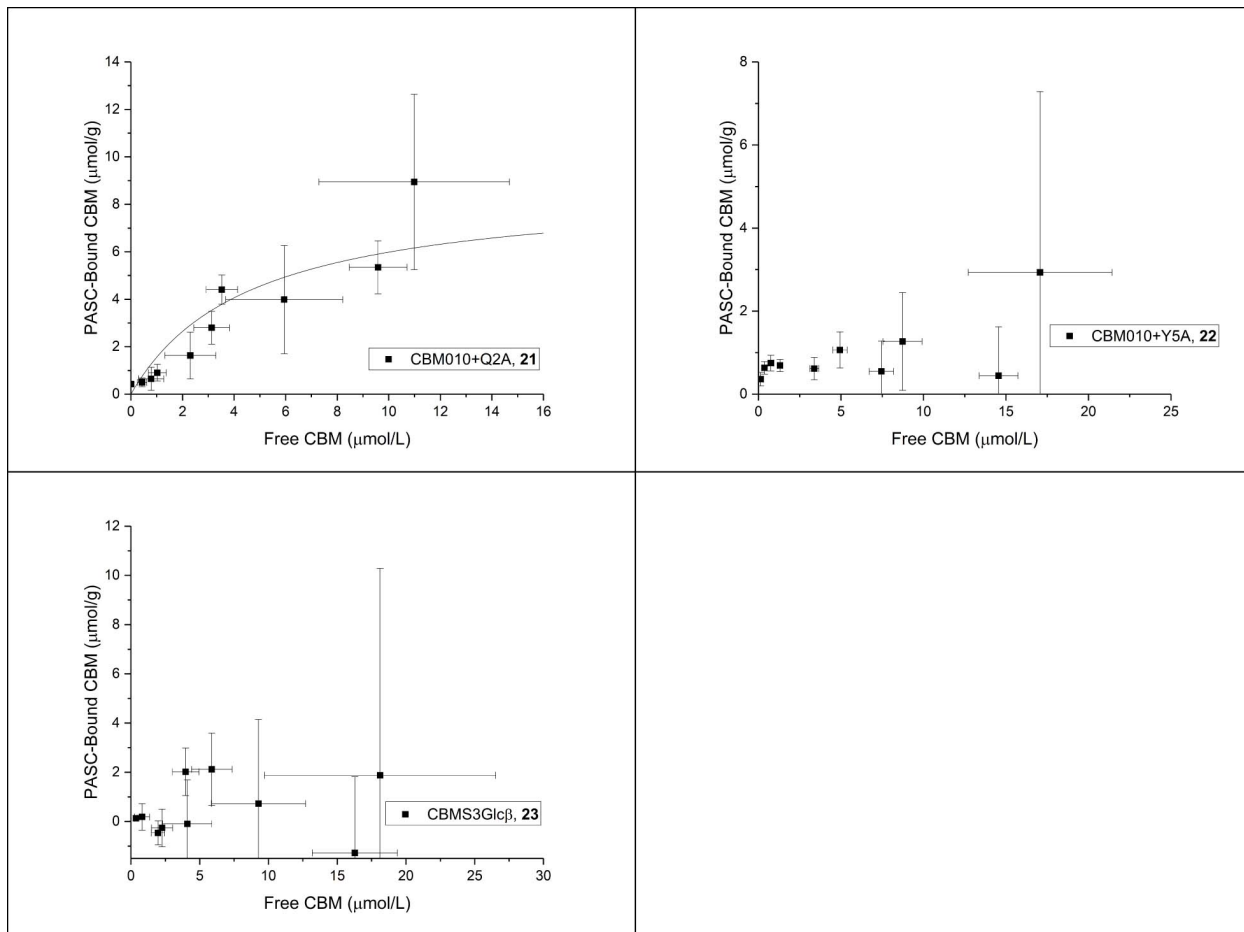
3. PASC at 4 °C



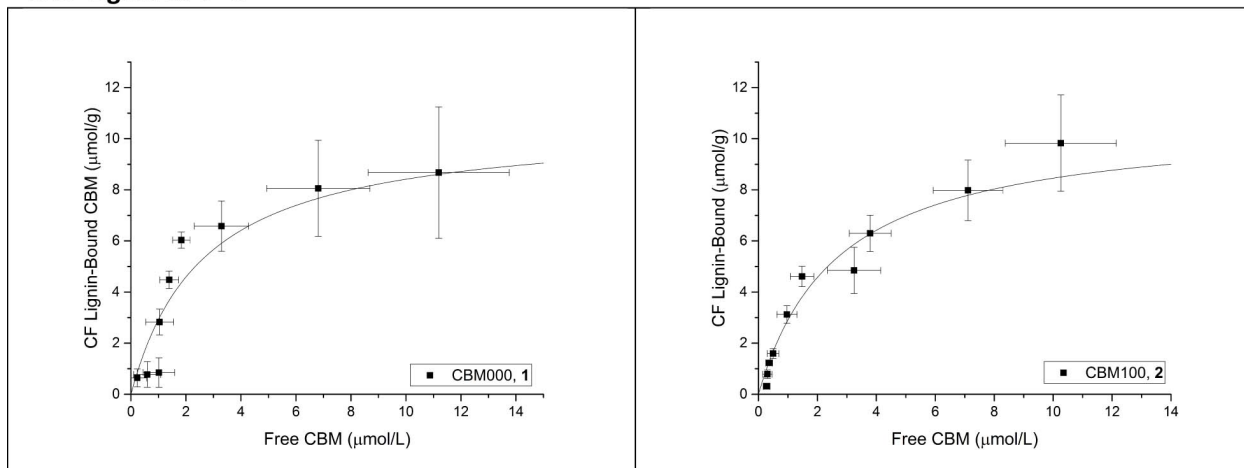


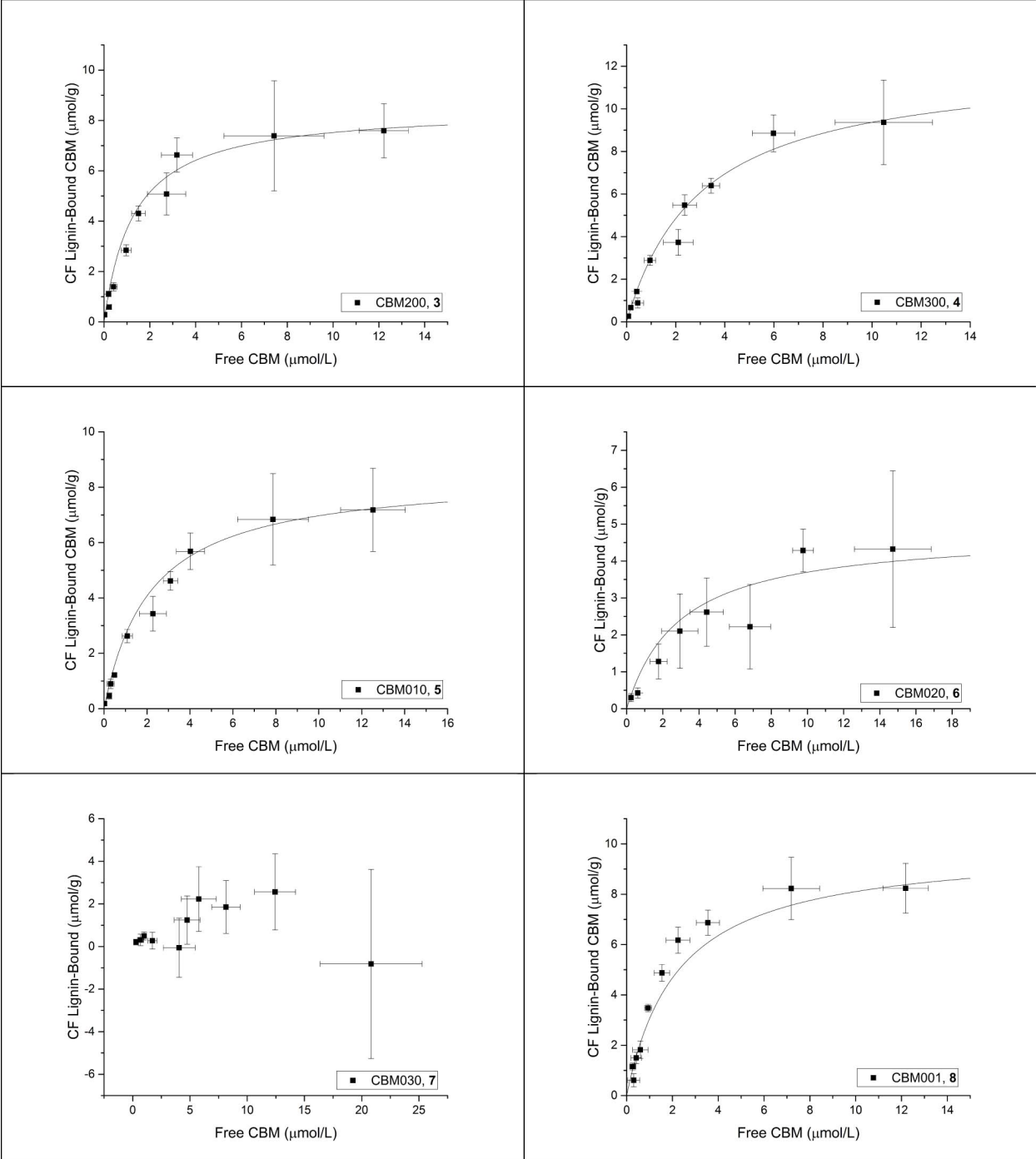


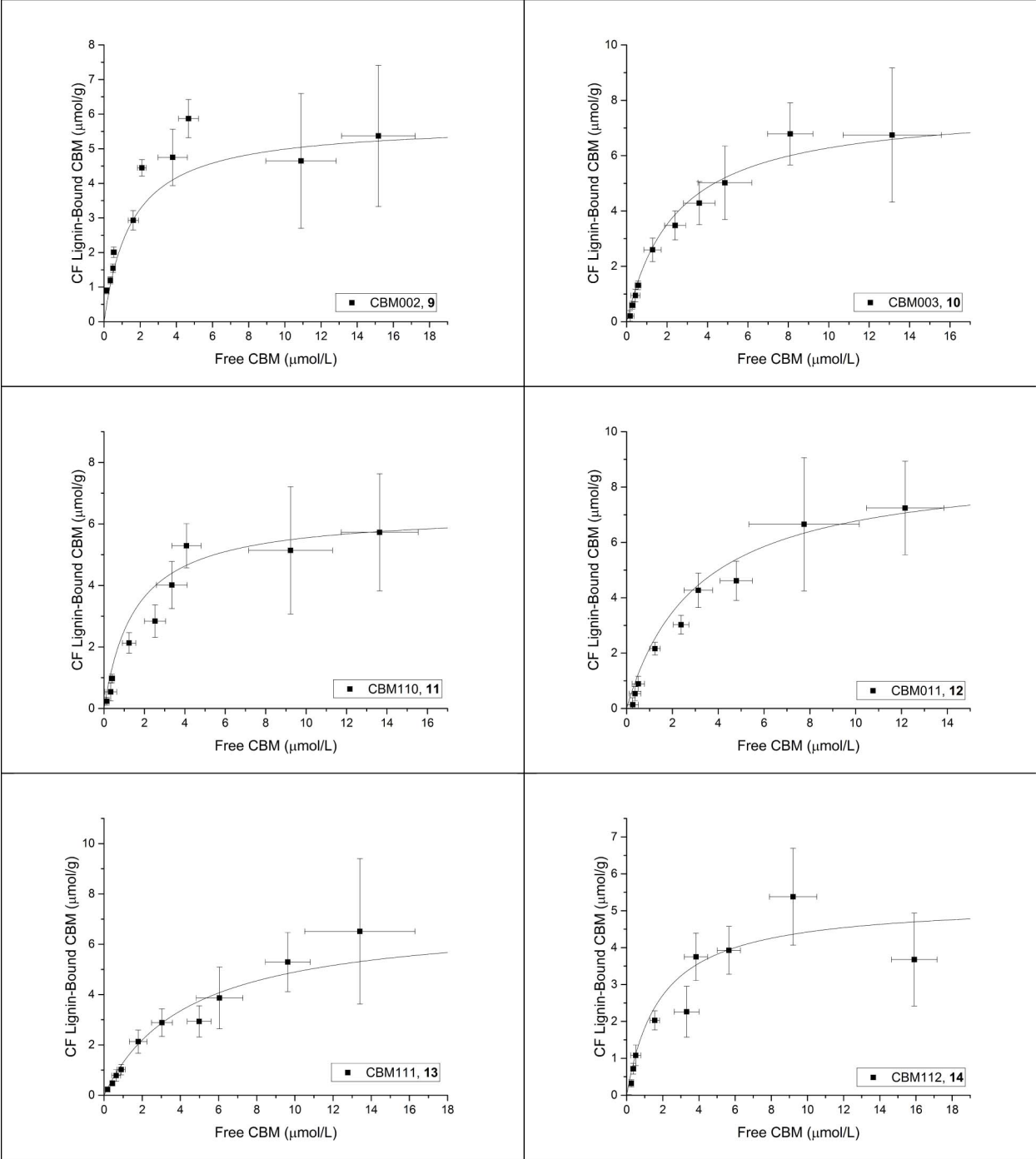


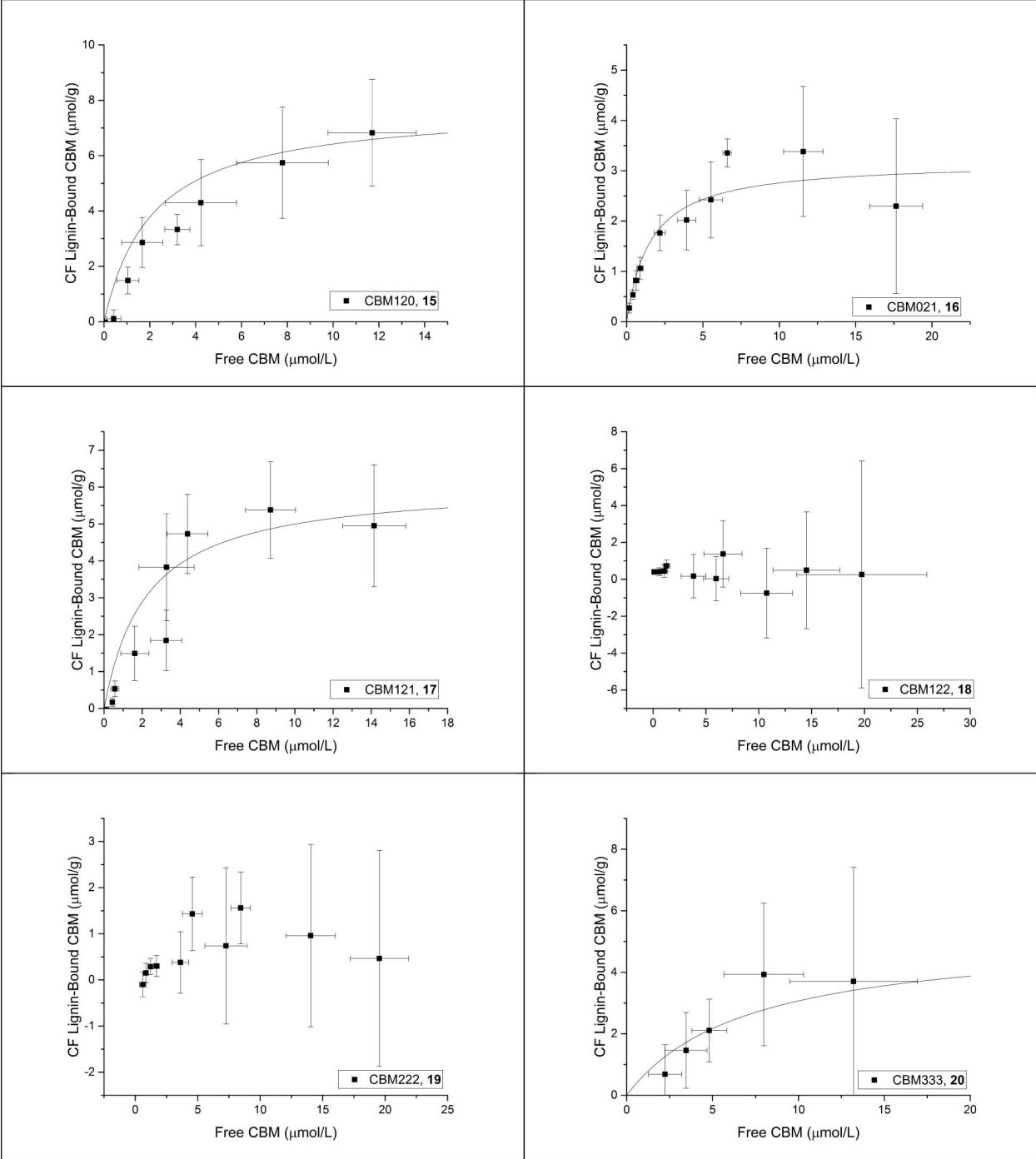


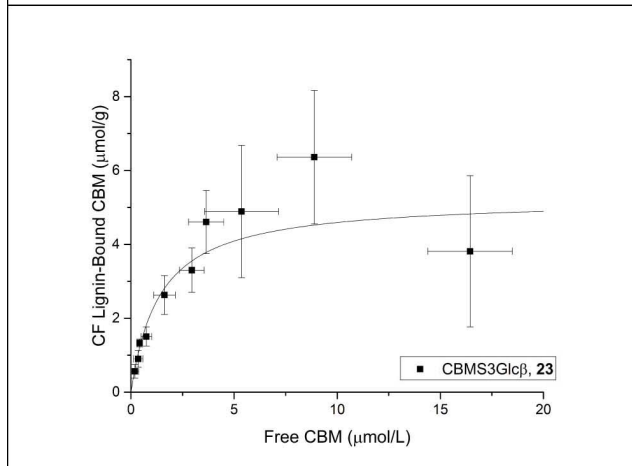
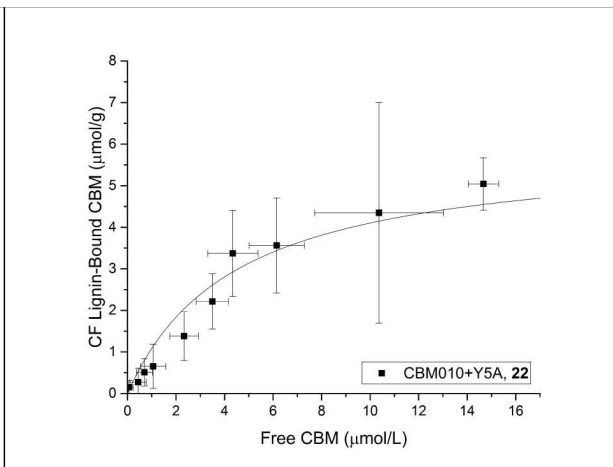
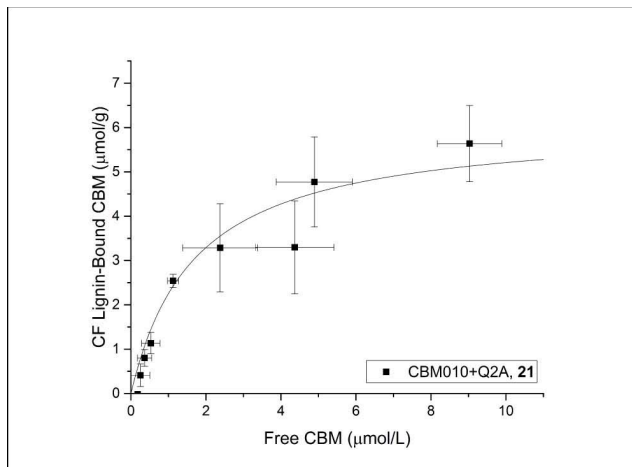
4. CF Lignin at 4 °C



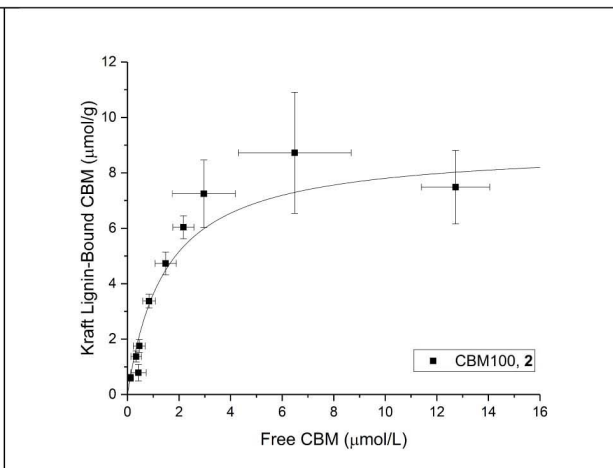
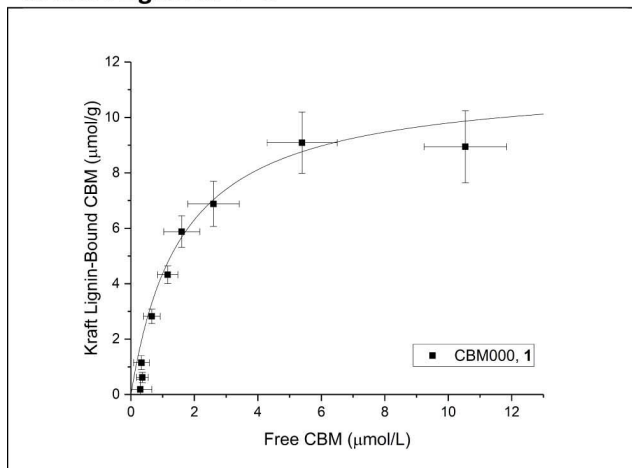


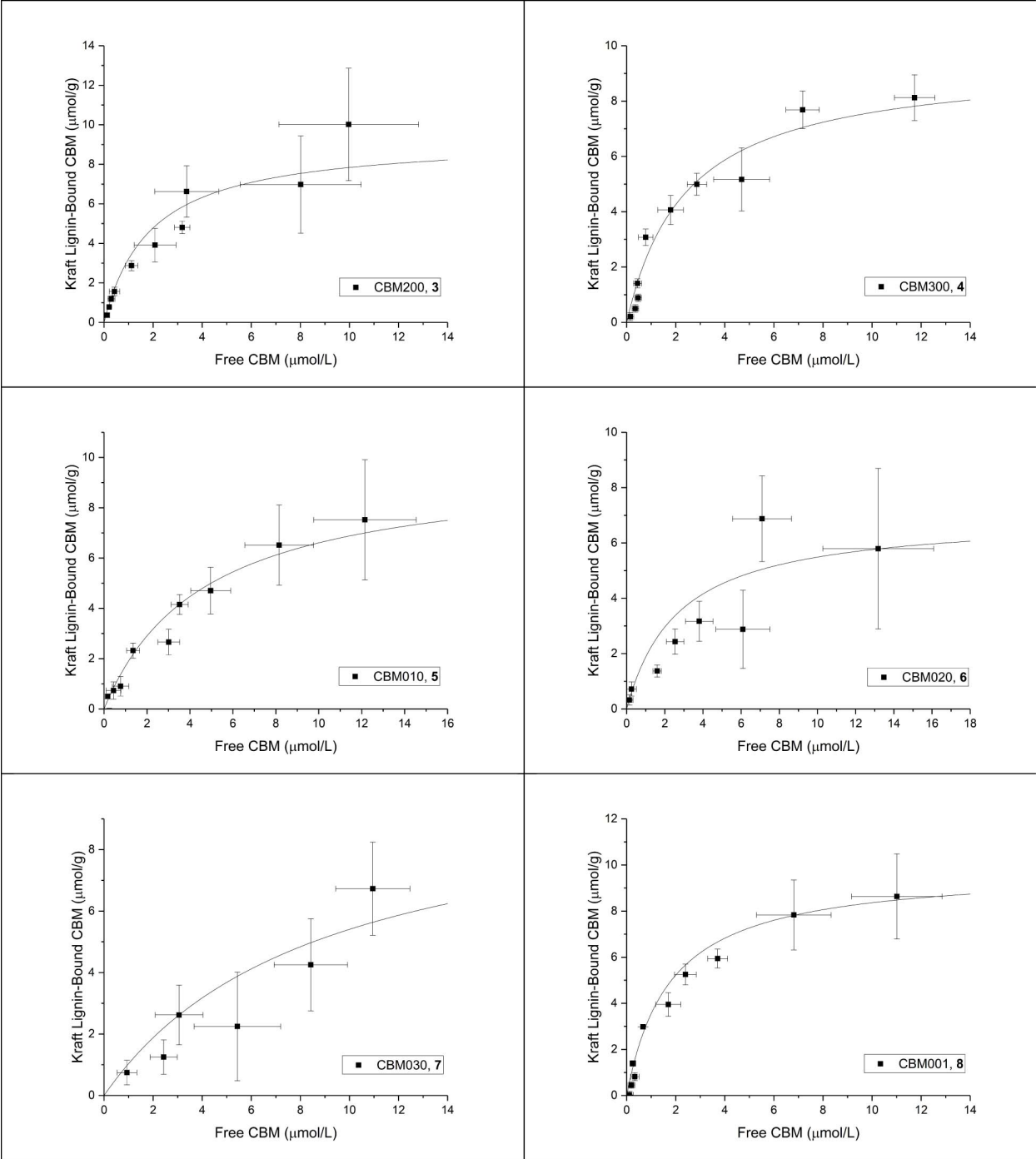


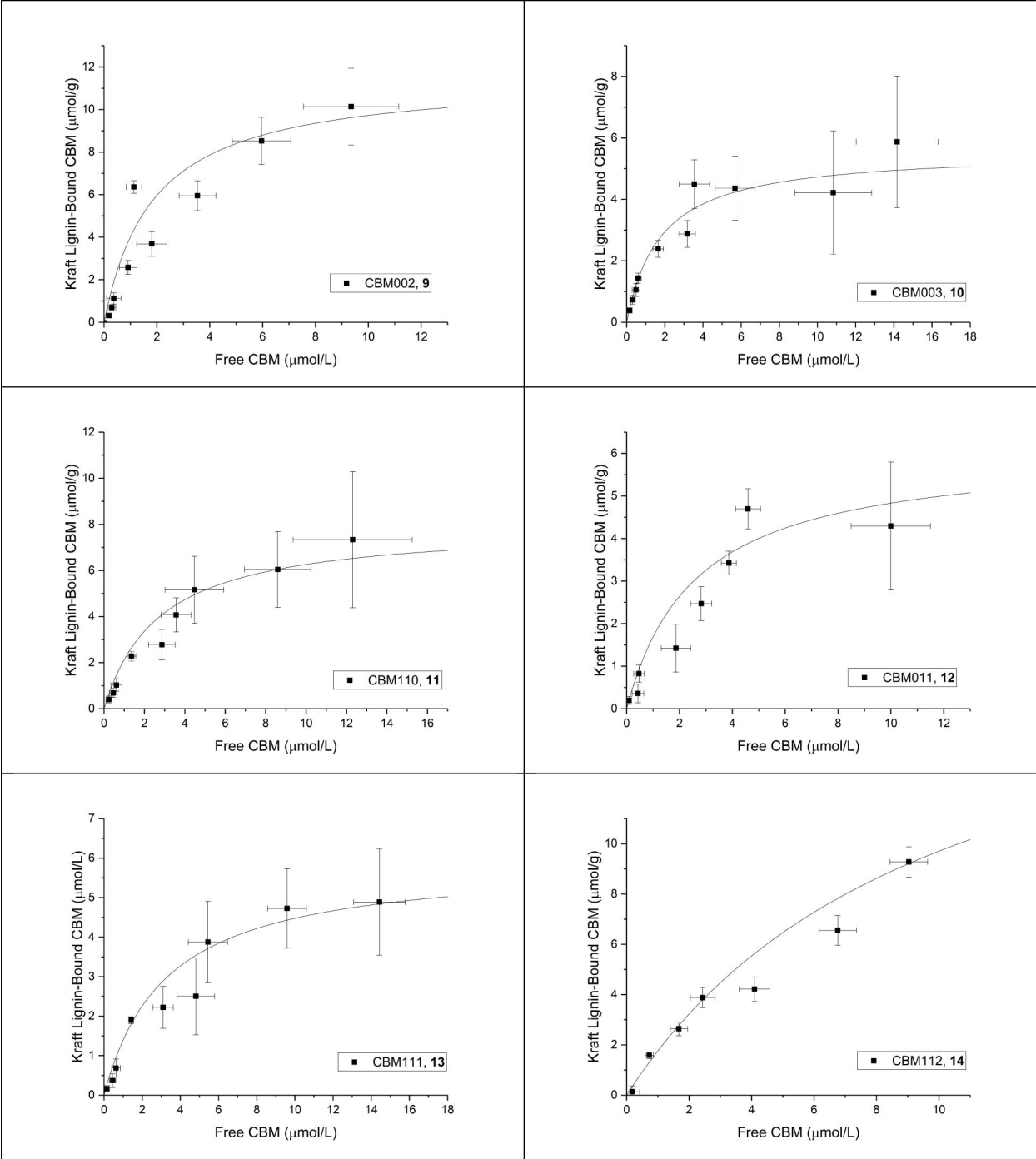


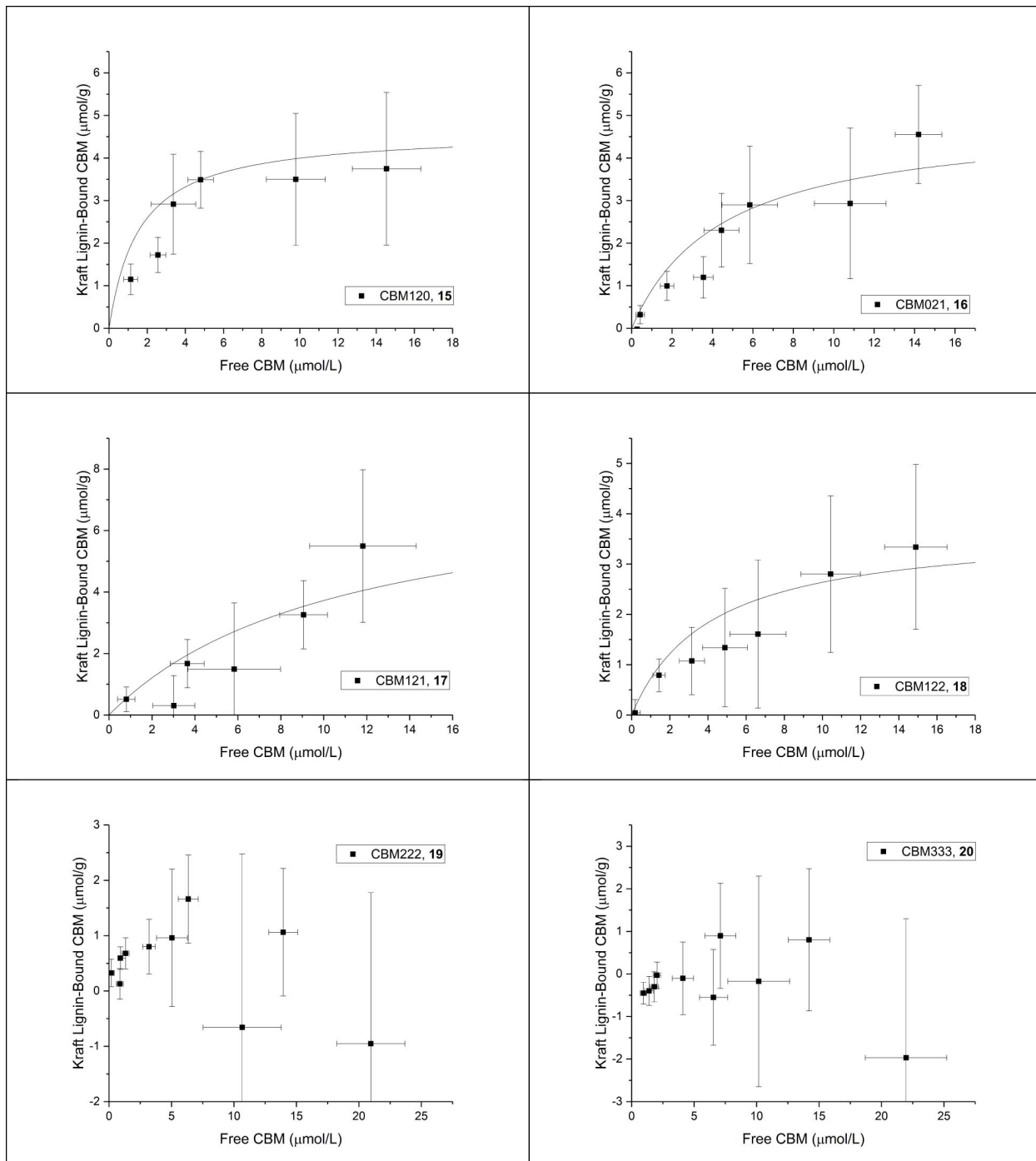


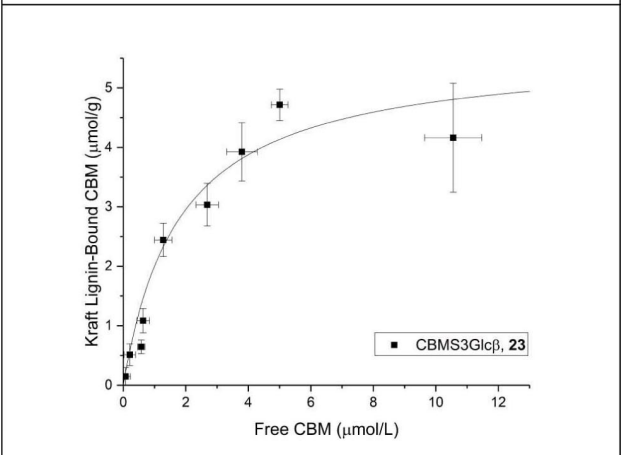
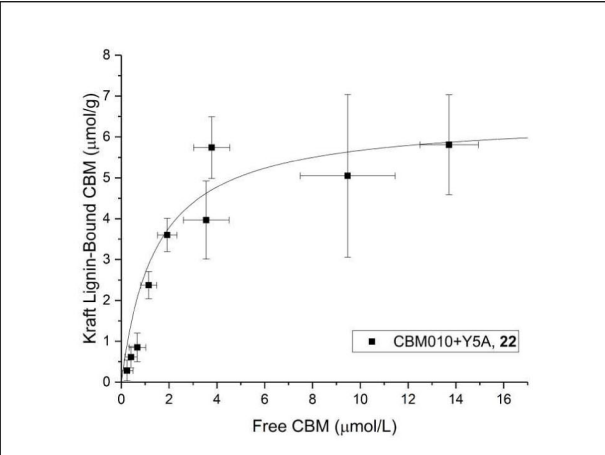
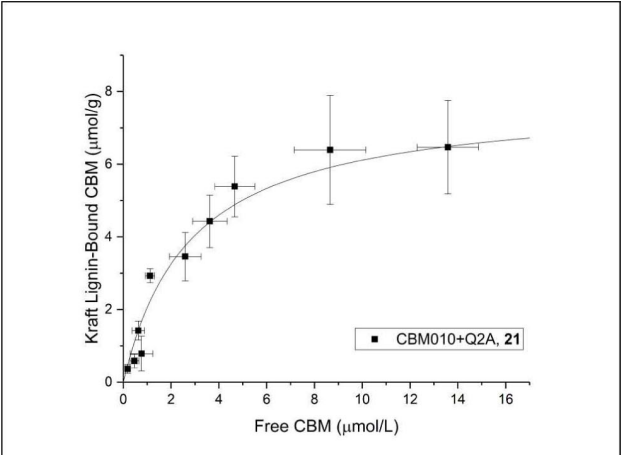
5. Kraft Lignin at 4 °C



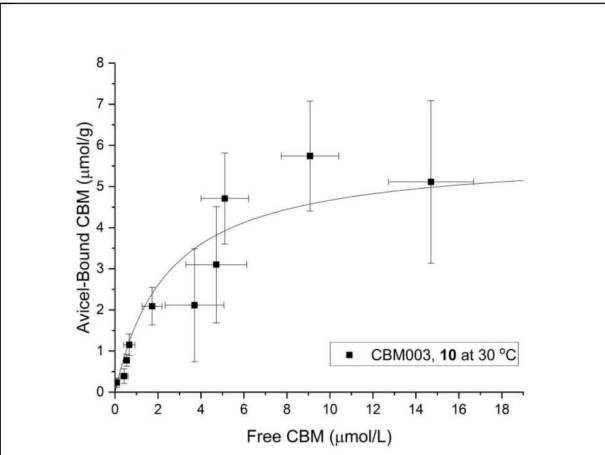
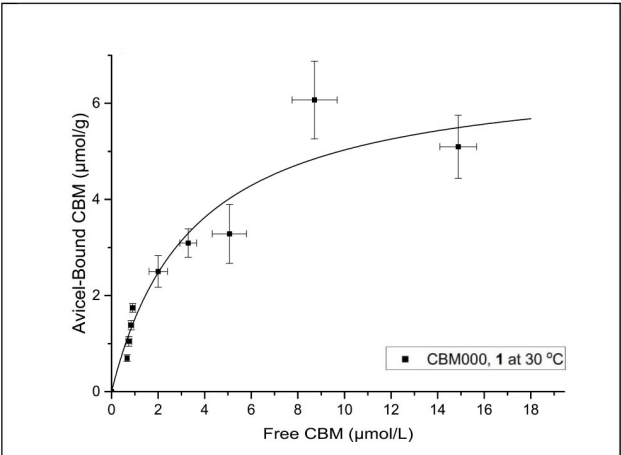


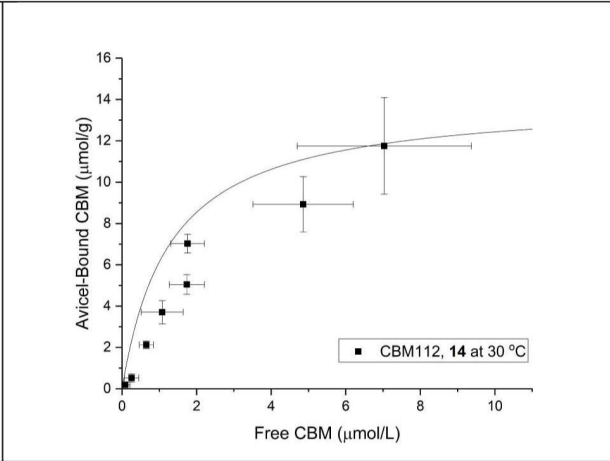
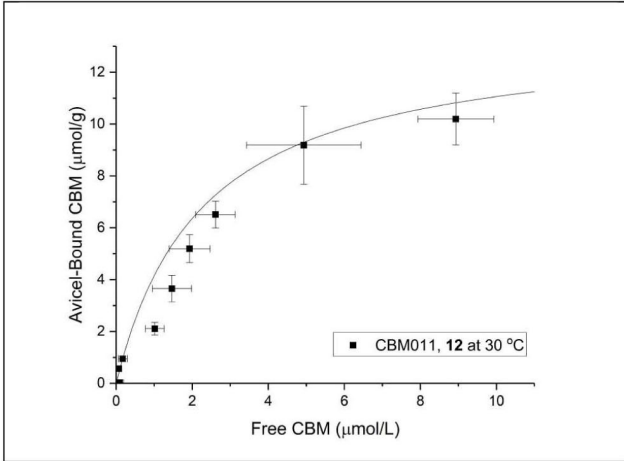




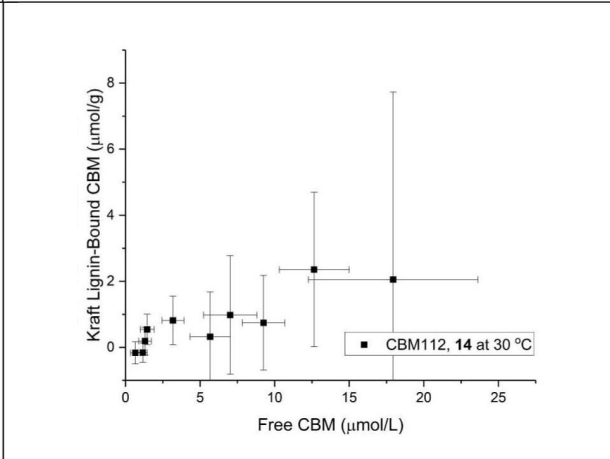
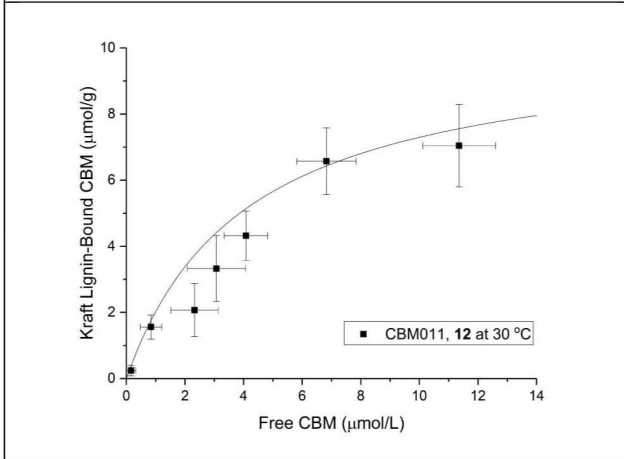
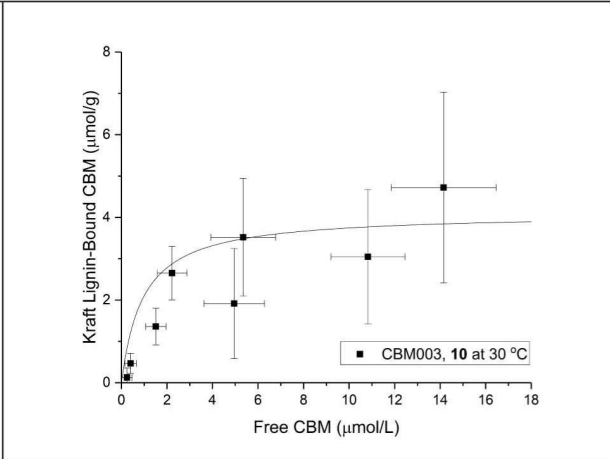
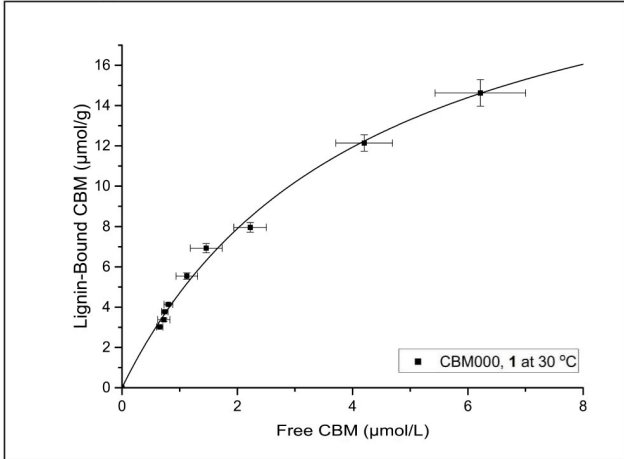


Avicel at 30 °C





Kraft Lignin at 30 °C



References:

1. Chen, L.; Drake, M. R.; Resch, M. G.; Greene, E. R.; Himmel, M. E.; Chaffey, P. K.; Beckham, G. T.; Tan, Z., Specificity of O-glycosylation in enhancing the stability and cellulose binding affinity of Family 1 carbohydrate-binding modules. *Proc Natl Acad Sci U S A* **2014**, *111* (21), 7612-7.
2. Guan, X.; Chaffey, P. K.; Zeng, C.; Greene, E. R.; Chen, L.; Drake, M. R.; Chen, C.; Groobman, A.; Resch, M. G.; Himmel, M. E.; Beckham, G. T.; Tan, Z., Molecular-scale features that govern the effects of O-glycosylation on a carbohydrate-binding module. *Chem Sci* **2015**, *6* (12), 7185-7189.
3. Hinkle, D. E.; Wiersma, W.; Jurs, S. G., *Applied statistics for the behavioral sciences* (5th ed.). **2003**.